

## TOPICAL REVIEW

# Ferromagnetic enhanced inductive plasma sources

Valery Godyak

RF Plasma Consulting and University of Michigan Brookline, MA, USA

E-mail: [egodyak@comcast.net](mailto:egodyak@comcast.net)

Received 11 March 2013, in final form 26 April 2013

Published 25 June 2013

Online at [stacks.iop.org/JPhysD/46/283001](http://stacks.iop.org/JPhysD/46/283001)

## Abstract

The subject of this paper is the review of inductively coupled plasma (ICP) sources enhanced with ferromagnetic cores, FMICP, found in various applications, including plasma fusion, space propulsion, light sources, plasma chemistry and plasma processing of materials. The history of FMICP, early attempts for their realization, some recent developments and examples of successful FMICP devices are given here. A comparative study of FMICPs with conventional ICPs demonstrates their certain advantages in power transfer efficiency, power factor and their ability to operate without rf plasma potentials at low plasma densities and with small gaps, while effectively controlling plasma density profile.

(Some figures may appear in colour only in the online journal)

## 1. Introduction

Plasma source development has been one of the major research activities in the low-temperature plasma community for several decades. It is primarily driven by the everlasting new requirement for applications. It is generally believed that different applications require different plasma properties, which is realized by the selection of different plasma sources. It is usually expected that the plasma property is inherently controlled by the specific method of plasma generation. In fact, the plasma parameters and rates of plasma processing produced by different plasma sources tend to be very similar to each other. This is because the plasma property is mainly controlled by the plasma geometry, gas composition, pressure, and power absorbed by the electrons [1, 2]. Therefore, for a given application, the most important features of a plasma source affecting the plasma processes are the characteristics of the boundary sheaths, plasma uniformity and the power delivering efficiency. In addition, the source should be able to operate over a wide range of power and gas composition.

Taking the application in microelectronics industry as an example, in the past few decades, a great variety of plasma sources has been considered for large scale semiconductor manufacturing. The main rf plasma sources under exploration have been the capacitively coupled plasmas (CCPs), including very high frequency CCPs (VHFCCPs), inductively coupled plasmas (ICPs), including ICPs enhanced by a ferromagnetic

core, helicons, electron cyclotron resonance (ECR) and surface wave (SW) plasmas [3, 4].

However, some of these sources suffer from some inherent disadvantages, which severely limit their performances in modern state-of-the-art applications. In the case of CCPs driven by 13.56 MHz, the major problem is the inability to generate high plasma densities at low gas pressures, and at high rf powers, they are mostly spent on ion acceleration rather than plasma generation. Although ICPs are used in many applications with high density plasmas, there are fundamental problems and drawbacks in their implementation for large-scale plasma processing systems. The low power factor of ICP antenna coil loaded with plasma ( $\cos\varphi \ll 1$ ) requires a resonant-matching network, and leads to relatively high power losses in the coil and the matching network. This diminishes the ICP power transfer efficiency and prevents ICP operation at low plasma density. Due to high coil voltage (reaching a few kV), an essential capacitive coupling exists between the coil and plasma. As a result, a considerable rf sheath develops on the plasma side of the window that separates coil and plasma which leads to intensive ion bombardment causing window erosion and plasma contamination. A transmission line effect developing along the ICP coil may also cause significant deterioration of plasma uniformity over the processing surface. Both capacitive coupling and the transmission line effect become growing problems for ICP with large processing areas, high power and high driving frequencies.

Even for VHFCCPs, which are today's mainstream approach for plasma etching reactors), there are some fundamental problems associated with the electromagnetic nature of the VHF field, as revealed by scientists and engineers in both industry and research laboratories. The problems are due to the finite skin depth (comparable to the plasma gap) or/and the standing wave effect [5–8]. They cause considerable plasma non-uniformity, which will become more severe for higher operating frequencies, higher plasma densities and larger wafer sizes. Furthermore, at very high frequencies, in a typical for CCP planar electrode structure, the inductive coupling may prevail over the capacitive coupling [7]. At very high frequency, various electromagnetic resonant modes may occur, depending on the rf frequency, the plasma size and the plasma density. In this case, VHFCCPs' operation may become unstable and uncontrollable due to mode jumping. From the production cost point of view, VHF rf generators and matching-tuning networks are expensive and have low power efficiency. For these reasons, it is my opinion that VHFCCP reactors have no future for 450 mm wafer or large panel processing.

In order to overcome the above-mentioned problems and to satisfy the requirement for uniform processing of large wafers with high speed, the following two design concepts have been proposed: (1) a low-frequency ICP enhanced by a ferromagnetic core (FMICP) [9–12] and (2) an ICP having multiple antennas to realize distributed rf excitations [13–15]. The first design concept has been inspired by the extensive research experience in the lighting industry. In fact, all existing commercial rf light sources are essentially low-frequency ICPs with ferromagnetic cores and are operated with extremely high efficiency [16]. However, many existing commercial ICP reactors for plasma processing are far from an optimal design and performance, and recent proposals (mainly in the patent literature) for their improvement by application of ferromagnetic cores did not bring any new viable ICP design.

A great number of books and reviews have been devoted to ICP basic properties, their physics and engineering [1–4, 16–24]. The subject of this paper is a review of ICPs enhanced with ferromagnetic cores, FMICPs, their history, some recent proposals, and some successful realizations. New unpublished results by the author are also included.

The structure of the review is as follows. In section 2, we consider the FMICP applications in fusion, lighting and plasma chemistry which demonstrate their advantages over traditional ICPs. A detailed comparative study of ICP and FMICP is given in section 3. In section 4, we analyse some recently proposed FMICP sources for large scale plasma processing. In section 5 we consider an advanced distributed FMICP with a controllable plasma profile. FMICPs with immersed rf couplers, some applications and specifics of FMICP operation in pulse mode are given in section 6. Concluding remarks are given at the end of the paper.

## 2. Some FMICP applications

In 1936, Bethenod and Claude [25] were the first to propose an enhanced ICP by placing a ferromagnetic core with a coil inside

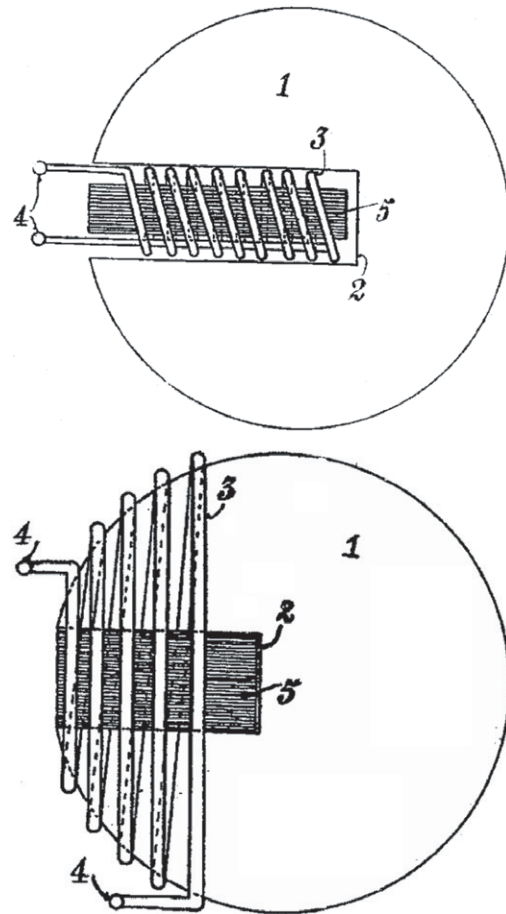


**Figure 1.** The first proposal of ICP with ferromagnetic core for lighting.

a spherical discharge glass vessel, as shown in figure 1. It was long before the development of contemporary technology for gas discharge light production, fluorescent and high intensity discharge (HID at high gas pressure). Half a century later, the first rf fluorescent lamp based on the proposal in [25] was unveiled by Philips [26]. This became possible because of the progress in semiconductor electronics and power switching technology, which led to efficient and cost effective rf power sources.

In the late 1950s, the very first practical application of FMICP was implemented in the toroidal plasma fusion devices (similar to today's tokamaks) for initial gas breakdown and its ionization followed by plasma heating and confinement. Such an approach is used in today's toroidal fusion facilities such as International Thermonuclear Experimental Reactor, ITER [27]. In those devices an ICP is maintained inside a metal toroidal chamber by electromotive force created by a time variable magnetic flux in the transformer steel core (magnetic circuit) that embraces the toroidal chamber, as shown in figure 2. The magnetic flux in the ferromagnetic core at low frequency (just a few periods of decaying oscillations) is created by discharging a powerful battery of capacitors to the primary winding of such a transformer. The stainless steel toroidal chamber wall with its thickness less than its skin depths, or with dielectric insertions in the chamber are used to ensure the magnetic field penetration into the metal discharge chamber.

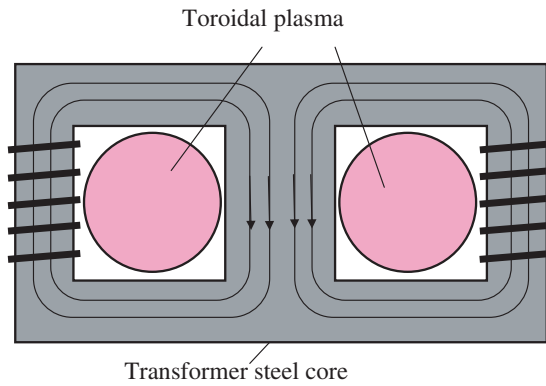


**Figure 2.** First application of ICP with ferromagnetic core in the toroidal plasma for fusion.



**Figure 3.** Endura/Icetron® powerful rf fluorescent lamps system.

More recently, different kinds of FMICP have been utilized in rf light sources [28–31] and in plasma-chemical reactors for generation of active processing gases and oxidation [32, 33]. In those FMICPs with rf power ranging between 20 W and 200 kW, the frequency between a few kHz and a few MHz at gas pressure from a fraction of mTorr to atmospheric pressure has been used. Let us consider in more detail some FMICP devices to demonstrate advantages of using ferromagnetic cores.

### 2.1. FMICP for light generation

Following the concept of toroidal plasma transformers for fusion, Bell [28] built an rf ion laser and Andersen [29] built an rf fluorescent lamp by closing the glass discharge tube upon itself forming a racetrack shape and surrounding it by toroidal ferrite cores with primary winding fed by an rf generator. However, those light sources showed poor performance, and the concept of toroidal plasma transformers was therefore not able to compete with traditional solution for lighting applications.

Just a quarter of a century later, it was shown [30] that, with optimal design, such an rf lamp can not only become a competitive product, but can exceed the performance of conventional (i.e. with electrodes) fluorescent lamps in efficiency and total light output. We are not aware of similar developments in lasers.

Developed at Osram Sylvania [30, 35], the powerful electrodeless fluorescent lamp Endura/Icetron® and its

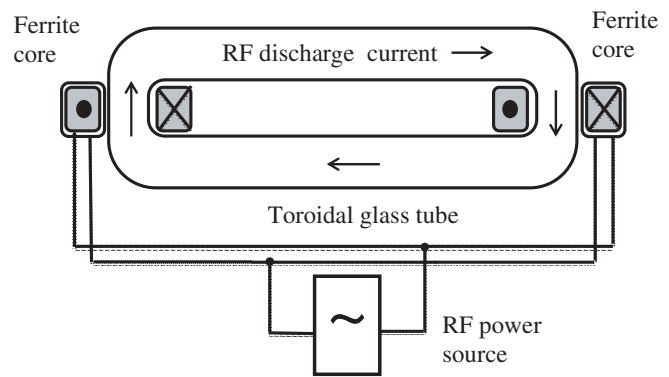


**Figure 4.** Schematic of Endura/Icetron® rf lamp.



**Figure 5.** QL rf fluorescent lamps of 165, 85 and 55 W.

schematic are shown in figures 3 and 4, respectively. A racetrack/toroidal shape glass tube having ID 5 cm with discharge path about 80 cm is filled with argon or krypton gas at a pressure of 0.3 Torr with mercury vapour at about 7 mTorr. The tube is covered inside with a phosphor converting the mercury resonance UV radiation into visible light. The electromotive force that maintains the plasma is induced by two ferrite toroidal cores with their primary winding connected to a high efficiency (90%) rf power converter (ballast) fed from the line voltage of 120 or 220 V.

The lamp operates at 250 kHz with consumed ac power of 150 and 100 W producing 12 000 and 8000 lm, respectively. At the discharge current of 6 A, the plasma density on the discharge axis of 150 W lamp is  $1.3 \times 10^{12} \text{ cm}^{-3}$  and the electron temperature is 1 eV. The unique feature of this FMICP lamp is the extremely high power transfer efficiency  $\eta$ , that is the ratio of the rf power absorbed by plasma to that delivered to ferromagnetic couplers from the rf source. The 150 W Endura/Icetron lamp has the record high power transfer efficiency ( $\eta = 98\%$ ), the highest among commercial rf plasma sources ever made. At  $\eta = 98\%$ , only 2% of rf power is lost in the ferrite couplers. Among others industrial FMICP devices, Endura/Icetron lamp has documented records of thorough experimental and theoretical studies of its light, electrical and plasma characteristics (including electron energy distribution functions (EEDFs) measurement) in both CW and pulse modes [35–38].

Another successful product based on FMICP is the Philips QL rf lamp [26] shown in figures 5 and 6. The lamp topology is the same as that of the Bethenod lamp [25], having a coupler (antenna) with ferrite rod immersed inside the lamp

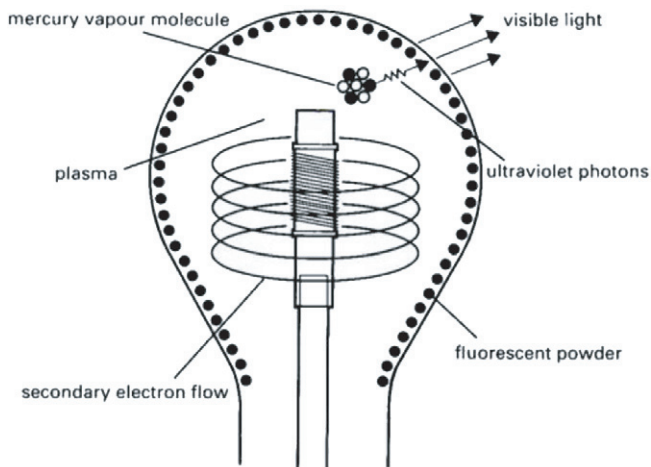


Figure 6. Schematic of QL rf fluorescent lamp.



Figure 7. Dura-One<sup>®</sup> compact rf fluorescent lamps.

bulb. Placing the ferrite antenna inside the plasma increases its coupling to plasma and prevents the obstruction of the generated light by the coupler set outside the lamp. The QL lamp operates at 2.65 MHz with an ac power of 85 W and light output of 6000 lm with power transfer efficiency  $\eta = 94\%$ . Note that the fraction of rf power lost in the couplers in the considered above rf lamps is an order of magnitude lower than that in conventional industrial ICPs for plasma processing of materials.

Later, the Genura<sup>®</sup> of General Electric [39] and the Dura-One<sup>®</sup> of Osram Sylvania [40] have both been developed as compact versions of rf fluorescent lamps suitable for replacement of incandescent and electroded fluorescent lamps. Two versions of the electromagnetic interference free compact rf lamp Dura-One are shown in figures 7 and 8. Both lamps have topologies similar to the QL lamp and operate at 2.65 MHz with ac powers of 20 W (A-shape) and 23 W



Figure 8. X-ray image of Dura-One lamp prototype.

(reflector type). Both versions of the lamp have light efficiency four times higher and longevity 15 times longer than those of incandescent bulbs. The power transfer efficiency in these lamps is over 90%.

Today, there is a great variety of commercial rf light sources utilizing FMICP and following the topologies considered above. Compact fluorescent rf lamps in the range 15–25 W suitable for replacement of low-efficiency and short-lived incandescent bulbs as well as very high-power rf fluorescent lamps (up to 1 kW) have been developed and commercialized by many US, European and Far East companies. The elimination of electrodes that are necessary in conventional gas discharge light sources allowed for flexibility in lamp shapes and for prolongation of lamp life up to 100 000 h.

## 2.2. Transformer coupled toroidal discharge TCTD

A variety of high power (0.1–200 kW) plasma sources based on FMICP in toroidal metal chambers (Tokamak type discharges, or Transformer Coupled Toroidal Discharges, TCTD) operating at relatively low frequencies (10–580 KHz), in the gas pressure range between  $10^{-4}$  Tor up to atmospheric pressure, have been developed for laboratory study and manufactured for different industrial applications as described in [32, 33, 41–46].

A review of the transformer coupled toroidal discharges TCTD developed in Russia has been recently published in [46]. Particularly, a detailed study of electrical, chemical and thermal characteristics of these devices has been considered in applications for plasma-chemical synthesis of NO and O<sub>3</sub>, as well as for UV and visible light generation.

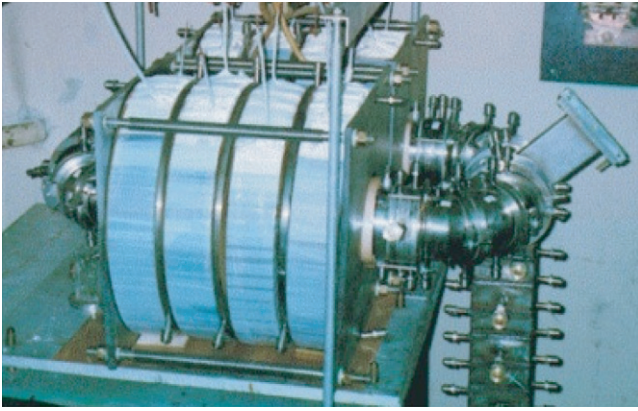


Figure 9. Powerful TCTD plasmatron driven at 10 kHz.

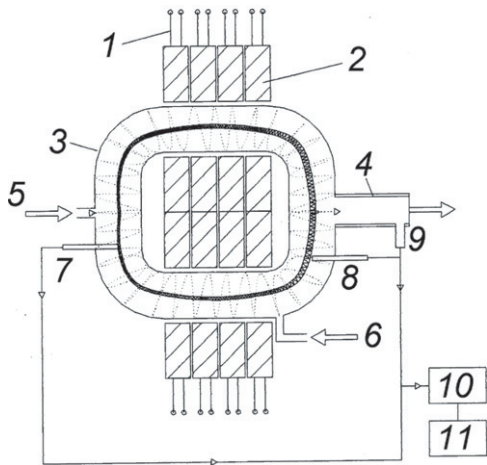


Figure 10. Schematic of a powerful TCTD experiment. 1—primary winding; 2—sections of magnetic core; 3—discharge chamber; 4—heat exchanger; 5—main gas feed; 6—secondary gas feed; 7—probe no 1; 8—probe no 2; 9—probe no 3; 10—spectrophotometer; 11—mass-spectrometer.

An example of such a device is a high-power plasma reactor operating at 10 kHz with maximal power of 180 kW that is shown in figures 9 and 10. High-density plasmas in noble and molecular gases were maintained in a water-cooled metal toroidal chamber consisting of several insulated sections and having inner diameter of 8–10 cm and perimeter of 180 cm. The ferromagnetic core consisted of eight-sections made of transformer steel sheet wound into toroidal shape having 42 cm OD, 16 cm ID and 7 cm height.

A similar TCTD, Astron<sup>®</sup> [33] operating as a remote plasma source for production of chemically active gases has been developed and manufactured by MKS. In this reactor, high density plasma in a molecular gas flow is maintained in a sectioned toroidal metal chamber encircled with closed-path ferrite cores with primary winding driven at 400 kHz with a few kW of rf power. Such a device usually dissociates molecular gases to obtain chemically active species for cleaning plasma processing chambers and/or treating of materials.

Nearly fully ionized pulse plasma has been obtained in pulse FMICP energized with a toroidal ferromagnetic inductor

immersed in the plasma chamber [47]. The six-turn primary winding of the inductor was switched by a thyatron to a pulse forming network. The induced plasma current in the chamber filled with xenon gas at a pressure range  $(1.0\text{--}3.3) \times 10^{-4}$  Torr reached up to 300 A during the 70–200  $\mu\text{s}$  pulse, producing plasma density up to  $10^{13} \text{ cm}^{-3}$ . The maximal power transfer efficiency in this device reached 90%.

The applications and devices considered above demonstrate the viability and attractive features of FMICPs, such as high efficiency and ability to operate at significantly lower driving frequencies than those usually used in plasma processing equipment at 13.56 MHz. Utilization of low frequencies for plasma generation allows for more efficient and less expensive power sources and facilitates the power management. Moreover, the direct drive (without rf or hf generator) of FMICP from the power line at 60 Hz has been demonstrated in laboratory experiment by Eckert [48].

### 3. Comparative study of ICP and FMICP sources

The FMICPs considered above do not give direct answers to the following question: what would be the performance of those ICP devices without ferromagnetic cores? Moreover, is there a quantitative characterization of the merit for adding a ferromagnetic core? The answers to those questions are extremely important for the development of new plasma sources. Those answers, however, are not trivial. It is not easy to produce (or realistically model) plasma sources with and without ferromagnetic core, which have the same geometry, gas pressure, frequency and discharge power, and thus, have the same plasma parameters. It is apparent that each of the mentioned characteristics (and all of them together) would affect the plasma source performance.

#### 3.1. The difference between conventional transformer and conventional ICP

In spite of common operational principles, there are fundamental differences in electrical properties of a conventional ac transformer and a conventional rf ICP. Due to a strong coupling between primary and secondary circuits ( $k \approx 1$ ) provided by a ferromagnetic core with closed magnetic path and high permeability  $\mu \approx 10^4$ , a conventional transformer behaves very closely to an ideal transformer, for which

$$k = 1, \quad Q_1 = \omega L_s / R_{12} \rightarrow 0, \quad \text{Cos}\phi = 1, \\ V_1 / V_2 = I_2 / I_1 = N_1 / N_2, \quad R_{12} = R_2 (N_1 / N_2)^2.$$

Here  $k$  is the coupling coefficient between primary and secondary circuits of the transformer,  $k = M(L_0 L_2)^{-1/2}$ ,  $M$  is the mutual inductance between the primary coil inductance  $L_0$  and the magnetic inductance  $L_2$  of the plasma current path (defined by its geometry),  $Q_1$  is the  $Q$ -factor of the primary circuit,  $L_s$  is the leakage inductance of the primary winding,  $R_{12}$  is the resistance  $R_2$  of the secondary circuit transformed to the primary circuit,  $V_1$ ,  $V_2$ ,  $I_1$ ,  $I_2$ ,  $N_1$  and  $N_2$  are, correspondingly, the voltages, currents and numbers of turns of the primary and secondary windings. Note that  $Q_1$

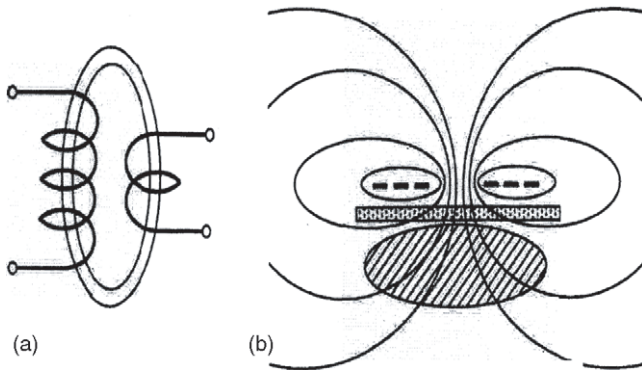


**Figure 11.** Magnetic line structure in a conventional transformer (a), and in a conventional ICP (b).

defines the ICP power factor  $\text{Cos}\phi = (1 + Q_1^2)^{-1/2}$ , and for  $Q_1 \gg 1$ ,  $\text{Cos}\phi = Q_1^{-1}$ .

In contrast, in a conventional ICP operating in rf frequency range with no core and loose coupling between coupler coil and plasma ( $N_2 = 1$ ,  $\mu = 1$ ,  $R_2 = R_p$ ):

$$k = 0.2-0.7, \quad Q_1 = \omega L_s / R_{12} \gg 1, \quad V_1 / V_2 \neq N_1$$

and  $R_{12} \neq R_p N_1^2$ .

Due to large  $Q$ -factor of the primary coil loaded with plasma, a resonant-matching network is needed to compensate the coupler coil reactance  $\omega L_s \approx \omega L_0$ , and to effectively transfer rf power from an rf generator to the antenna coil. The large resonant coil current  $I_1$  (in the range of tens of ampere) and coil voltage  $V_1$  (in the range of a few kV) in the typical plasma processing equipment lead to a considerable power loss in both the coil and the matching network. For this reason, the power transfer efficiency of a conventional ICP is essentially lower than that of the conventional ac transformer. Recall that the efficiency  $\eta = 98\%$  of Endura/Icetron rf lamp mentioned in section 2.1 is higher than the efficiency of a regular ac transformer of similar power.

Figure 11 illustrates the principal difference between a regular transformer and a conventional ICP. In a regular transformer, due to a closed ferromagnetic core with high permeability, practically all the magnetic flux, created by the primary winding, is inside the core and crosses the secondary winding, and vice versa. As a result, the transformer is very close to an ideal transformer with the secondary load  $Z_2$  being transformed to the primary circuit merely as  $Z_2(N_1/N_2)^2$ .

In the conventional ICP, the magnetic flux, created by the primary coil, spreads out, and its significant portion does not embrace the nearby plasma, but instead closes upon itself in the space between the plasma and the coil. Similarly, the magnetic flux created by the plasma current is loosely coupled with the ICP inductor coil. As a result, the ICP coupling coefficient  $k$  is essentially less than 1, making the conventional ICP a merely poorly performing transformer.

### 3.2. Power transfer efficiency

The power transfer efficiency  $\eta$  is the ratio of rf power  $P_p$  absorbed by plasma to the power delivered to the coupler coil  $P$ ,  $\eta = P_p / P = (1 + \tau)^{-1}$ , where  $\tau = P_c / P_p$  is the relative

coil loss and  $P_c$  is the power loss in the coupling inductor  $P_c = P - P_p$ . An analysis of ICP system that accounts for coupler coil electrical parameters showed that the relative coupler power loss of the ICP system  $\tau$  is given by the following expression [49]:

$$\tau = P_c / P_p = (k^2 Q_0 Q_p)^{-1} [(Q_p + \omega / \nu_{\text{eff}})^2 + 1],$$

where  $Q_0 = \omega L_0 / R_c$  is the  $Q$ -factor of the primary coil (coupler) with no plasma,  $Q_p = \omega L_2 / R_p \propto P_p$ ,  $R_c$  is the coupler resistance,  $R_p$  is the plasma resistance, and  $\nu_{\text{eff}}$  is the effective electron collision frequency which accounts for both collisional and stochastic (collisionless) rf power absorption [50–52].

Note that in general, the coupler power loss  $P_c$  is defined by the power lost in the ferromagnetic core material  $P_f$  and the power  $P_w$  lost due to the winding rf resistance  $R_w$ , thus  $P_c = P_f + P_w$ . It follows from the expression above that  $\tau \propto (k^2 Q_0)^{-1}$ . Hence, to minimize coupler loss, one has to increase the coupling coefficient  $k$  and its  $Q$ -factor  $Q_0$ , and to operate at the lowest possible rf frequency ( $\omega < \nu_{\text{eff}}$ ). At relatively low discharge power, when the plasma  $Q$ -factor is  $Q_p = \omega L_2 / R_p < (1 + \omega^2 / \nu_{\text{eff}}^2)^{1/2}$ , the relative coil loss is dropping with increase in  $Q_p$ . Since  $R_p \propto P_p^{-1}$ , it follows that  $Q_p \propto P_p$ , and the relative coil loss is falling with the discharge power. On the other hand, an increase in plasma resistance  $R_p$  leads to an increase in the relative coupler loss. For those reasons the conventional industrial ICP reactors working with molecular and electronegative gases (having intrinsically high plasma resistivity) cannot operate in the ICP mode at relatively low plasma density.

The limitation on the minimal rf power (and thus, plasma density) at which stable ICP operation in inductive mode is possible is defined by the power lost in the coupler  $P_c$ . An empirically found rough criterion of ICP stability is  $P_c < P_p$ , or  $\eta > 1/2$ , although, an ICP operation may be possible at  $P_p < P_c$  (but not at  $P_p \ll P_c$ ) when the coupler/matcher network has some ballasting feature.

In general, the coupler power loss is

$$P_c = I_1^2 R_w + A \zeta(B, F) = P_w(I_1) + P_f(V_1),$$

where  $R_w$  is the coil rf resistance,  $A$  is the ferromagnetic core volume,  $\zeta = \zeta(B, F)$  is the specific power loss of ferromagnetic material,  $B$  is the average over the volume magnetic induction in the core and  $F = \omega / 2\pi$  is the cycle frequency. Since the coupler voltage  $V_1 \propto BF$ , the power loss in the core is defined by the coupler voltage,  $P_f = P_f(V_1)$ , while the power loss in the coil is defined by the coupler current,  $P_w = P_w(I_1)$ .

According to ionization and electron energy balance of steady-state gas discharge plasma [4], the plasma sustaining rms electric field  $E$  is

$$E^2 = 3T_e m \xi \nu_{\text{eff}} (1 + \omega^2 / \nu_{\text{eff}}^2) / 2e \approx E_{\text{dc}}^2 (1 + \omega^2 / \nu_{\text{eff}}^2),$$

which is practically independent of the discharge power and the plasma density (what is nearly proportional to the discharge power  $P_p$ ). Here,  $T_e$  is the electron temperature in energy

units (eV),  $-e$  and  $m$  are the electron charge and its mass,  $\xi$  is the frequency of electron energy loss due to different kinds of collisions and electron escape to the wall and  $E_{dc}$  is the electric field rms in the self-sustained dc current plasma. Due to effects of the two-step ionization via excited states, and the dependence of the electron energy distribution on the plasma density, the electric field is slowly dropping with rf power (a well know feature of negative volt–ampere characteristic of gas discharge plasma).

Since the coupler rf current  $I_1$  is proportional to the electric field at the plasma boundary ( $E \propto I_1\omega$ ), the power lost in the coupler coil is  $P_w \propto E^2 \approx E_{dc}^2(1 + \omega^2/v_{eff}^2)$ . On the other hand, the coupler voltage  $V_1$  that defines the core loss is also proportional to  $E$ , while the power loss in the core  $P_f$  is growing with the coupler voltage faster than quadratic. Particularly, for ferromagnetic cores in FMICP applications,  $P_f \propto V_1^k$ , with  $k$  being between 2.1 and 2.9, depending on the material, frequency, magnetic induction strength and temperature.

The consequence of the coupler loss correlation with the plasma electric field (that is maximal at low plasma densities) is that in negative molecular gases with high electric fields, typical in plasma processing, the coupler power loss is excessively high. In such cases, the coupler loss needed to maintain the plasma may exceed the power capability of the available rf power source, and the plasma cannot be sustained. This problem can be avoided using FMICP which considerably reduces coupler power losses.

### 3.3. Effect of ferromagnetic core

The expression for the relative coil loss  $\tau$  suggests a way to reduce the coupler loss by increasing the plasma  $Q$ -factor  $\propto L_2$  using a high permeability ( $\mu \gg 1$ ) ferromagnetic core. The introduction of ferromagnetic core also increases the primary inductance  $L_0$  and the coupling between the coupler and plasma. The increase in the coupler and plasma inductances is defined by the effective permeability of the ferromagnetic core  $\mu_{eff} = L_c \setminus L_0$ . An increase in primary coil inductance  $L_0$  reduces the primary current by a factor of  $\mu_{eff}$  and reduces coil wire loss by a factor of  $(\mu_{eff})^2$ . Although an additional loss appears due to core loss, it can be made reasonably small with a proper choice of the core size, rf frequency and ferromagnetic material.

The core effective permeability  $\mu_{eff}$  may be much smaller than the ferromagnetic material permeability  $\mu$ . For closed magnetic path toroidal ferromagnetic cores with  $\mu \geq 10^3$  used in TCTDs, the value of  $\mu_{eff}$  is close to  $\mu$ . For cylindrical rods with  $\mu \geq 20$ , the value of  $\mu_{eff} \approx 1 + 2l_c/d_c$  is practically independent of  $\mu$ ; here  $l_c$  and  $d_c$  are the core length and diameter. For a single wire or flat winding unilaterally covered with ferrite slate,  $\mu_{eff} = 1.5$ – $2$ .

The most effective way to increase ICP performance is to use a high permeability core with a closed magnetic path. In this case,  $\mu_{eff} \approx \mu$ , the coupling coefficient is very close to unity ( $k \cong 1$ ), and the FMICP acquires many features of an ideal transformer. The possibility to drastically reduce the driving frequency (up to ac line frequency) is the most remarkable feature of a FMICP with a closed ferromagnetic

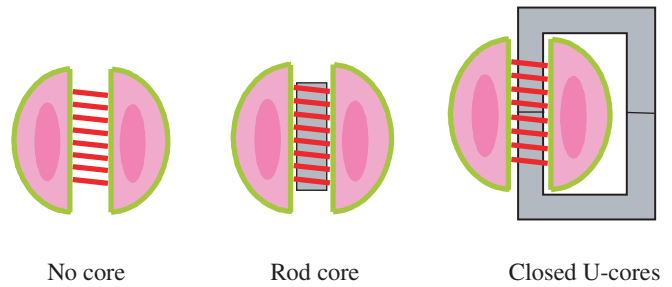


Figure 12. ICP sources with different couplers.

core. Unfortunately, the toroidal discharge current path in such FMICPs puts essential limitations on plasma configurations, thus limiting their applicability.

The performance comparison of three different ICP rf lamps of system power of about 150 W, operating at different frequencies and having different rf field configurations, has been reported in [31]. Three lamps were compared: the Endura/Icetron lamp with closed ferrite toroids, the QL<sup>®</sup> lamp with an internal coil and ferrite rod and the QL bulb energized by equatorial winding without a ferrite core, driven at 0.25 MHz, 2.65 MHz and 10 MHz, respectively. It has been found that the relative coupler power loss  $\tau$  for these lamps corresponded to 2.1%, 4.8% and 9.1% of the total system power. This result clearly shows the advantages of using ferromagnetic cores, especially those with a closed magnetic path.

### 3.4. Experiment with ICP of different coupler structures

A detailed comparison of electrical parameters of ICP without a core and with different ferrite core configurations, but with the same discharge geometry, the same rf field topology, and the same driving frequency, has been carried out by this author and partially published in [11]. The ICP electrical characteristics were measured in a wide range of discharge powers  $P_p$  (the power consumed by the plasma) that has been found as the difference between the total power and the power lost in the coupler. The ICP electrical characteristics were compared for the same plasma geometry and discharge power to obtain identical plasmas for different couplers.

Three ICPs with different coupler cores were sustained in a glass vessel formed by a spherical bulb (7.5 cm OD) and an inner tube (2.2 cm ID) housing the coupler. The vessel was filled with krypton–mercury mixture (0.5 Torr/6 mTorr) typical of fluorescent light sources. The ICPs were driven at 2.5 and 0.4 MHz with a 13-turn coil and different coupler configurations: with no core, with a ferrite rod core ( $l_c = 4.4$  cm,  $d_c = 1.85$  cm,  $\mu = 100$  for 2.5 MHz and  $\mu = 2000$  for 0.4 MHz) and with closed magnetic path formed by two ferrite U-cores of the same materials. In the discharge power range between 2.5 and 200 W, the volume average plasma loading was between 0.015 and 1.2 W cm<sup>-3</sup>. The three ICP configurations with different couplers are shown in figure 12. The results of the measurement are presented in figures 13–18.

The coupler winding current  $I_1$  and voltage  $V_1$  measured over a large range of discharge power, for three ICP

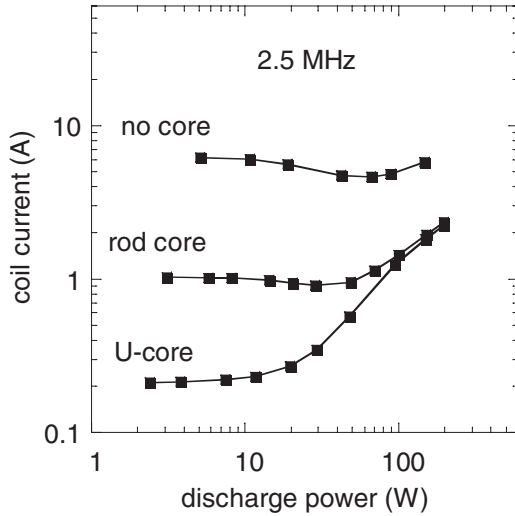


**Figure 13.** Coupler coil current as a function of discharge power at 2.5 MHz.

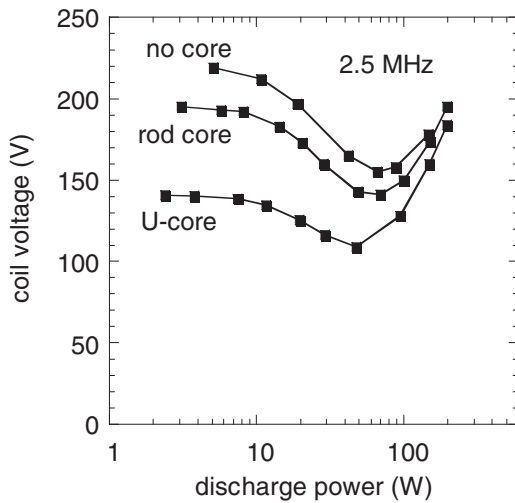


**Figure 14.** Coupler voltage as a function of discharge power at 2.5 MHz.

configurations are shown in figures 13 and 14. As seen in figure 13, the introduction of the ferrite rod dramatically ( $\mu_{\text{eff}}$  times) reduces the coupler current. Even a larger reduction in the coupler current occurs with the closed ferrite core. At small discharge powers (i.e. low plasma density), the values of the coupler current tend to the magnetizing currents  $I_0$ . At large discharge powers ( $P_p \geq 100$  W), the ICP sources with the rod core and the closed core operate like a conventional transformer with the  $I_1 \gg I_0$  when  $I_1 \approx I_p/N_1$ , where  $I_p$  is the plasma discharge path current.

The comparison of the coupler voltages, for different ICP configurations, given in figure 14, shows that introducing a ferrite core reduces the needed coupler voltage to maintain the same value of electromotive force (discharge voltage) in ICP. This is due to the increase in the coupling between the coupler and plasma. The fractions of the primary magnetic flux linked to the plasma, for the air-core, rod core and U-core are 0.63; 0.72 and nearly 1.

The falling of the coupler voltage with discharge power, seen in figure 14, reflects the negative  $I/V$  plasma discharge

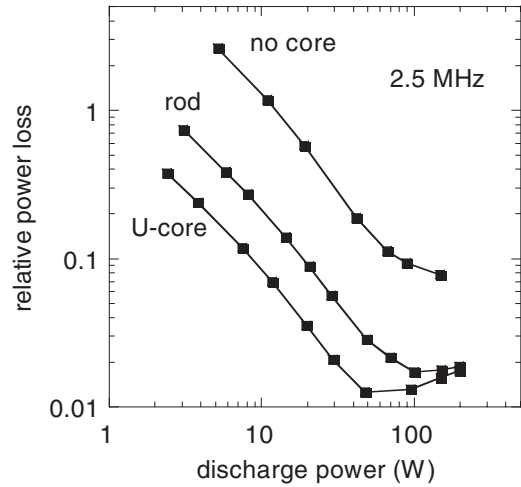


**Figure 15.** Relative coupler power loss as a function of discharge power at 2.5 MHz.

characteristic. On the other hand, the coupler voltage is growing at a large discharge power due to ballasting action of the plasma inductance  $L_2$  and the leakage inductance  $L_s$ , which is the portion of the coupler inductance not coupled to the plasma. Those two inductances and their reactances are practically independent of discharge power and plasma density, while plasma resistance is inversely proportional to plasma density and to discharge power. The resistive part of the plasma voltage stays nearly constant, while the voltage due to leakage and plasma inductances grows proportionally to the plasma current. For this reason, the rise in the coupler voltage takes place at the large discharge power.

A remarkable feature of FMICP is the dramatic reduction in the coupler loss compared with an ICP without ferromagnetic core. The relative coupler power loss  $\tau = P_c/P_p$  shown in figure 15 demonstrates an order of magnitude reduction in the coupler loss in the ICP with ferromagnetic core. According to the above expression,  $\tau$  drops with discharge power (since  $P_p \propto Q_p$ ), reaching its minimum at  $\omega L_2 \approx R_p \propto E/P_p$  for sufficiently large discharge powers. When a ferrite core is present, the increase in the plasma inductance  $L_2$  shifts the position of minimal  $\tau$  to a lower discharge power, see more details in [49]. The relative inductor loss in FMICP is an order of magnitude lower than in the ICP with no ferrite core, and at  $P_p = 100$  W,  $\tau \approx 1\%$ . This is 10 times less than in the best helicon plasma source which is considered to be the most efficient plasma source. The measured lowest antenna loss in the helicon plasma found in the literature is 10% [53].

Application of ferromagnetic core leads to a significant increase in the loaded with plasma coupler power factor  $\text{Cos}\phi$ , as shown in figure 16. In general, the power factor grows with  $\mu_{\text{eff}}$  and with discharge power, reaching its maximum at  $\omega L_2 \approx R_p$ , which for a closed ferromagnetic core approaches unity. As the power grows further,  $\text{Cos}\phi$  is dropping due to the increasing role of the leakage and plasma inductances at large plasma density.

A relatively high  $\text{Cos}\phi$  in FMICP allows for a significant simplification and for power loss reduction of the matching network, and eliminates the need for its resonant tuning. In

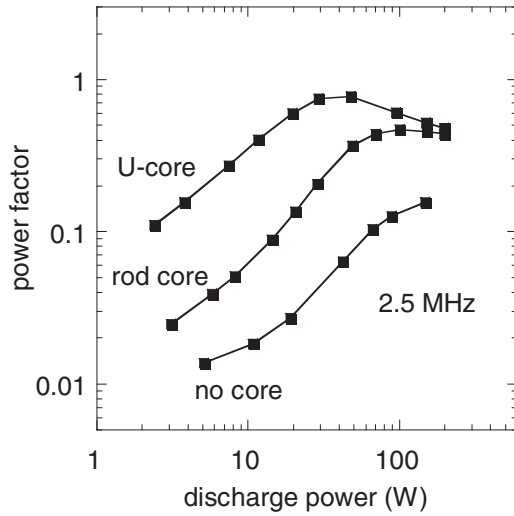


Figure 16. Power factor as a function of discharge power at 2.5 MHz.

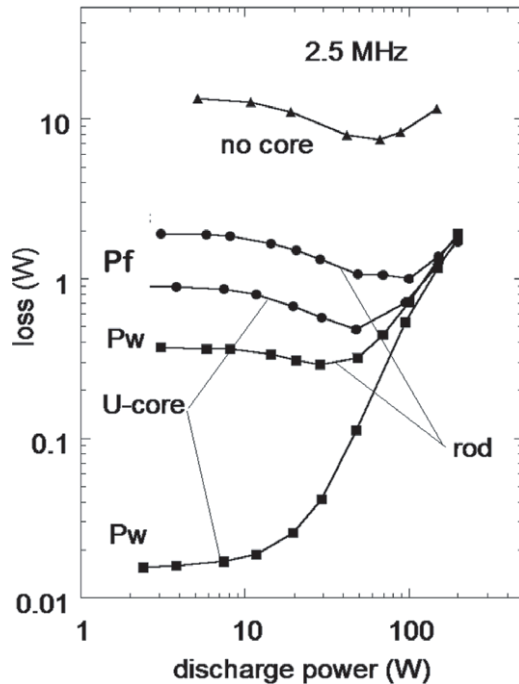


Figure 17. Power lost in winding  $P_w$  and in ferrite core  $P_f$  at 2.5 MHz.

fact, there is no need in a matching network at all for FMICP with a closed magnetic path, when  $\text{Cos}\phi \approx 1$ , and the matching can be achieved just by a proper choice of turns of the coupler winding.

Absolute power losses in the coupler winding  $P_w$  and in the ferrite core  $P_f$  are shown in figure 17. The wire power loss  $P_w = I_1^2 R_w$  remains around 10 W in all ranges of the discharge power for the ICP without a ferrite core, while  $P_w$  is negligible in the FMICP. Thus, at  $P_p = 10$  W, the wire power loss  $P_w$  in the FMICP is reduced 34 times for the rod core and 720 times for the closed core. Only at sufficiently large coupler currents does the wire power loss become comparable to the core loss.

Similar experiments carried out at 400 kHz are illustrated in figures 18–20. They show an even more dramatic difference

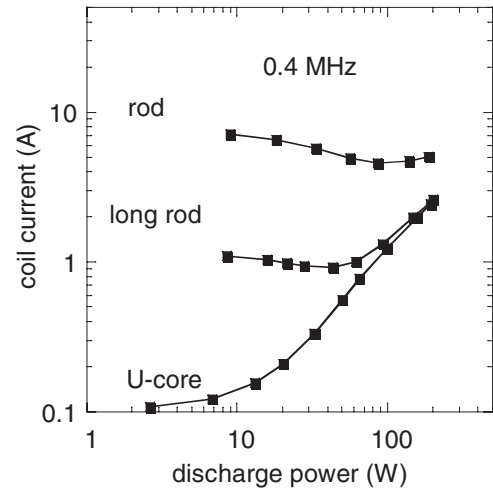


Figure 18. Coupler coil current as a function of discharge power at 400 kHz.

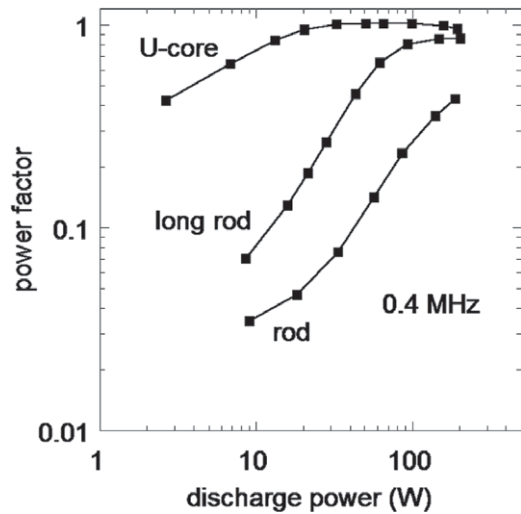
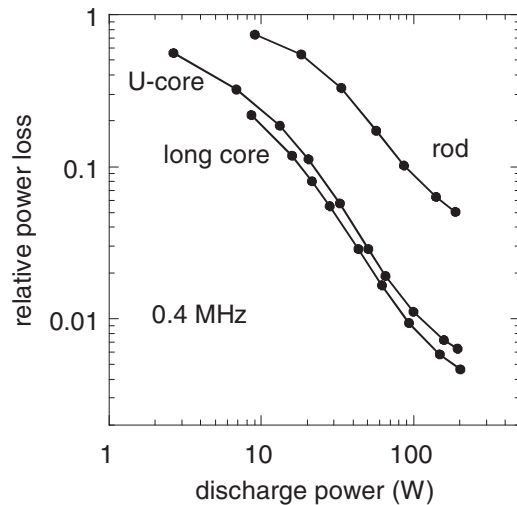


Figure 19. Power factor as a function of discharge power at 400 kHz.

between FMICP and conventional ICP. Note that at 400 kHz, it was impossible to maintain an ICP without a ferromagnetic core in this experimental arrangement. In fact, it can be shown that in order to maintain a 20 W ICP without a ferromagnetic core, about 40 A of coil current and 250 W of coil power loss are needed. Experiments at 400 kHz also have shown that the most efficient configuration of the coupler was the S-shaped long core formed by two U-cores of which one was turned at  $180^\circ$  around the discharge axis. In this case, the core loss reduction was due to a weakening of the magnetic flux at the core ends, in contrast to a closed ferromagnetic core where the magnetic flux along the closed path remains essentially unchanged.

Figure 18 shows the coupler current as a function of discharge power and demonstrates a stronger current reduction caused by the ferromagnetic core than the one found at 2.5 MHz. This difference is caused by the core with  $\mu = 2000$  instead of  $\mu = 100$  at 2.5 MHz. Similarly, the power factor given in figure 19 and the relative coupler power loss given in figure 20 are larger than those found at 2.5 MHz. Thus, the



**Figure 20.** Relative coupler power loss as a function of discharge power at 400 kHz.

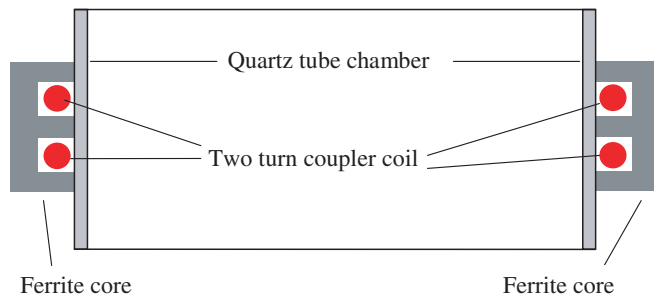


**Figure 21.** Schematic diagram of the FMICP with side antenna having ferromagnetic core.

power factor  $\text{Cos}\phi$  is practically equal to 1 in the discharge power range between 20 and 200 W for the closed U-core as seen in figure 19. At a maximal power of 200 W, the relative coupler loss  $\tau$  (shown in figure 20) for the closed U-core as well as for the long rod core is about 0.5%.

Comparing the  $\text{Cos}\phi$  and  $\tau$  values obtained in the 100 W FMICP at 400 kHz with the corresponding values in the 100 W ICP at 2.5 MHz without a core, we see a 7.5 times and a 20 times improvement.

#### 4. FMICPs for plasma processing

In this section, we consider a variety of recently proposed schemes aimed to improve ICP mainly for plasma processing applications. In particular, we will discuss specific features and limitations of different designs of FMICP for large scale processing.

##### 4.1. FMICPs with open ferrite core

The effect of adding a ferrite core to the coil coupler (antenna) in a cylindrical ICP driven at 13.56 MHz has been reported in [34]. A qualitative FMICP diagram of this experiment is shown in figure 21. A two-turn coil around the discharge chamber formed with 10 cm OD Quartz tube was covered with a ferromagnetic ( $\mu = 80$ ) belt as shown in figure 21. Electrical

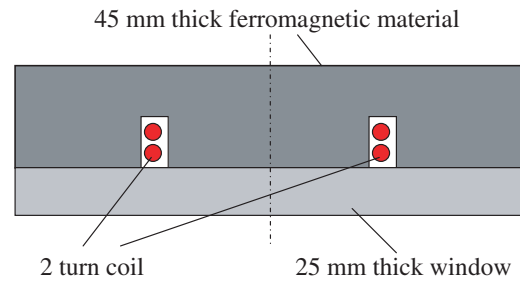


**Figure 22.** Schematic diagram of the FMICP with top antenna having ferromagnetic core.

and plasma parameters of this ICP with and without ferrite core were measured in the range of applied power between 25 and 500 W, at argon pressures between 5 and 20 mTorr.

The addition of ferrite core resulted in about 1.5 time reduction of the coil current and about 10% rise in both the coupling coefficient and the plasma density. The expected nearly two-fold reduction in the coil loss due to the current reduction was offset with the additional loss in the ferrite core. The reasons for a marginal improvement in the ICP characteristics with addition of the ferromagnetic core in this experiment are typical for other published works on FMICP and will be discussed later.

Electrical and plasma characteristics of an ICP with a top flat window and the coupler formed with a coil embedded in a ferromagnetic plate, as shown in figure 22, were reported in [9, 12]. The ICP parameters were measured at a driving frequency of 13.56 MHz in the input power range between 100 and 700 W, with and without the ferromagnetic core. Similarly to the results found in [34], the coil current was measured to be about 50% less than without the core. The reduction in the coil current should reduce the power loss in the coil and in the matching network, but additional power loss in the ferromagnetic core may offset this gain and even increase the total coupler loss. According to [9] ‘Nevertheless, reliable measurements of the power transfer efficiency have not been possible because of the poor measurement accuracy close to the 90°-shift phase’. However, given the fact of the thick window and of the very high power loss in the used ferromagnetic material at 13.56 MHz, one could expect the power transfer efficiency to be no better (or even worse) than without a ferromagnetic core.

The reduction in the window thickness to 4 mm (instead of 25 mm) resulted in a significant rise in the ICP efficiency, but the coupler arrangement had to be placed into a vacuum discharge chamber, to preserve the mechanical integrity of the window. Indirect efficiency assessment obtained by comparing the ion current with the probe installed in the chamber showed that (at the same input power) the ion current in FMICP with a 4 mm window is about four times larger than in the ICP with 25 mm window. A nearly similar result has been obtained in [12] for a large area ( $1 \times 1 \text{ m}^2$ ) FMICP with embedded coils and a thin window. However, to what extent this difference is attributed to the thin window or/and to the ferromagnetic core remains unclear.

Another scheme of FMICP for large area processing has been proposed and studied in [54, 55]. A typical device

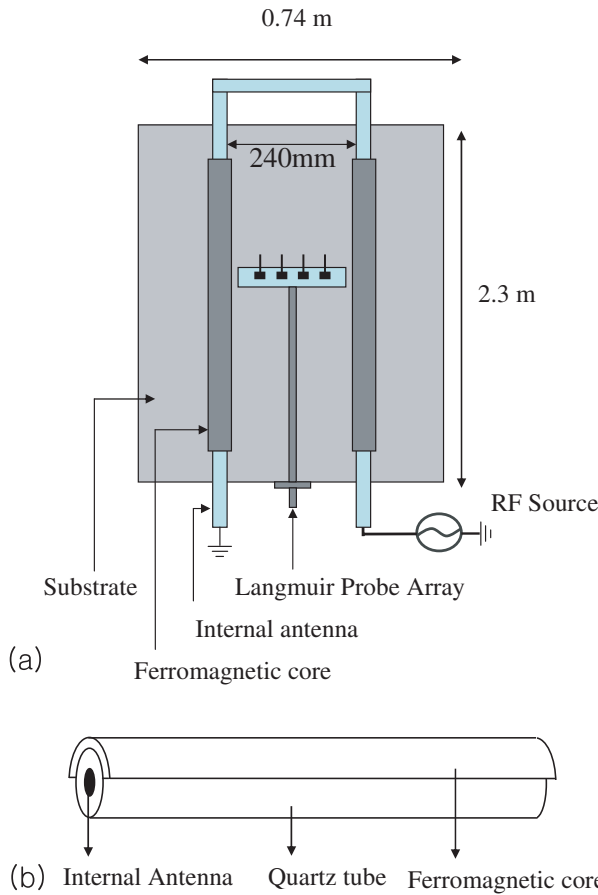


**Figure 23.** FMICP with immersed U-shaped antenna partly covered with ferromagnetic core.

used in those works is shown in figure 23. An immersed (internal) U-shaped antenna is covered with a quartz tube, then with a half-tube (inversed gutter) ferrite shield, and the entire structure is encapsulated in another quartz tube to protect the ferrite shield from chemical interaction with plasma.

Conceptually this approach is similar to the one used in [9, 12, 34]. The main idea was to reduce the magnetic resistance of the magnetic field path around the antenna conductor, in order to enhance the magnetic induction between ferrite poles in the gap facing the plasma. But using a thin wall quartz tube (instead of a thin large window in [9, 12]) to separate the coupler from the plasma simplifies the antenna construction and provides a more reliable mechanical integrity.

A detailed study of the electrical and plasma parameters for this kind of FMICP operating at 13.56 and 2 MHz, with and without a ferrite core, was performed in [54, 55]. The antenna current, voltage and power factor measured at 13.56 MHz and at argon pressure of 20 mTorr are shown in figure 24. As shown in figure 24, the application of a ferromagnetic core resulted in practically no change in the coupler voltage, in about 50% reduction in the coupler current and in doubling of the coupler power factor. The latter is due to enhancements in the coupling coefficient and in the additional power loss in the ferrite material of the antenna covered with the ferrite shield.

The reduction in the driving frequency to 2 MHz in this immersed coupler FMICP resulted in about three times reduction in the antenna power loss as shown in figure 25.

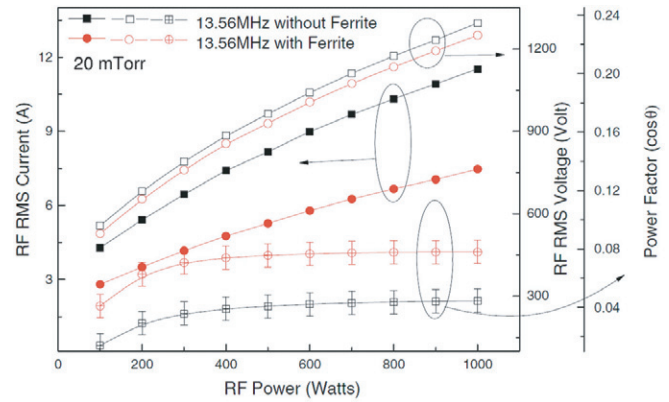


**Figure 24.** Voltage, current and power factor measured with and without ferromagnetic core.

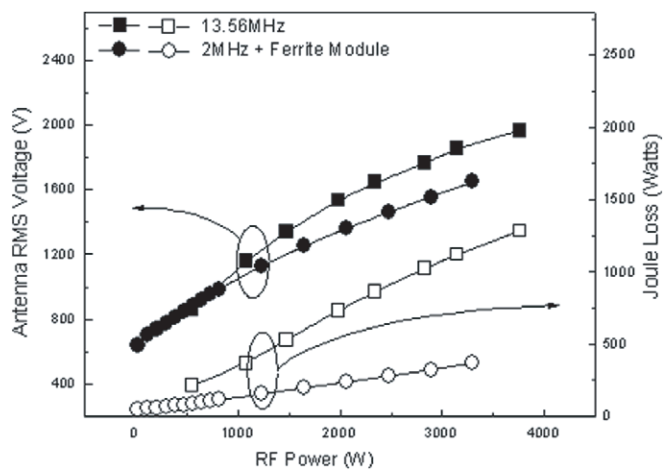


**Figure 25.** Comparison of the coupler voltage and coupler loss at 13.56 and 2 MHz in immersed FMICP.

This reduction is mainly due to reduced power loss in the ferrite shield which had an excessive loss at 13.56 MHz. Reduction in the driving frequency also resulted in the lowering of the plasma rf potential as shown in figures 26.

The three considered schemes of ICPs with ferromagnetic core demonstrate some marginal improvement in ICP source electrical and plasma characteristics. However, the modest 1.5 times reductions in the coupler current and some increase in the plasma density hardly justify the application of a ferromagnetic core in the ICPs built according to these schemes.

The common problem of those FMICP operating at 13.56 MHz is the use of ferromagnetic materials which causes excessive losses at this frequency, offsetting the expected positive effects of using a ferromagnetic core. The difference in ICP parameters measured at 13.56 MHz and in FMICP at 2 MHz may be mostly due to the combined effect of the difference in frequencies, and of the application of a ferromagnetic core. The other common and significant problem in the FMICP embodiments of [9, 12, 34, 54, 55] is the very small distance between the coupler poles compared with the distance to the plasma. That makes the majority of the rf magnetic flux to be closed in the window rather to embrace the nearby plasma (as shown in figure 27) and has a consequence of poor coupling. The resolution of this problem will be given later.

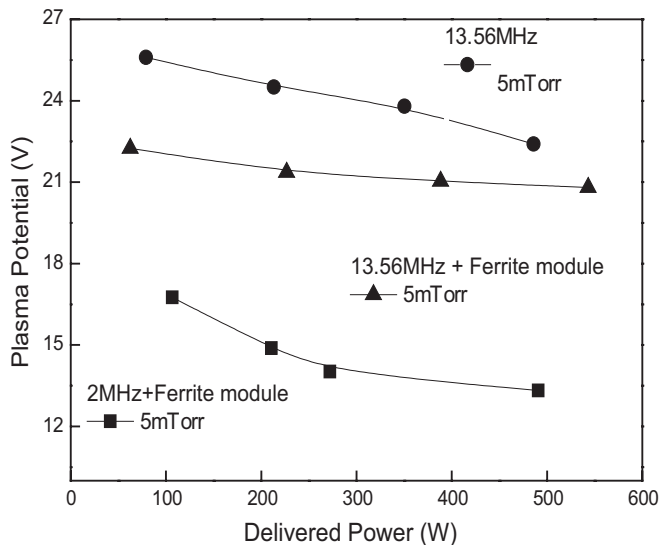


Figure 26. Plasma potentials without and with core at 13.56 and at 2 MHz.

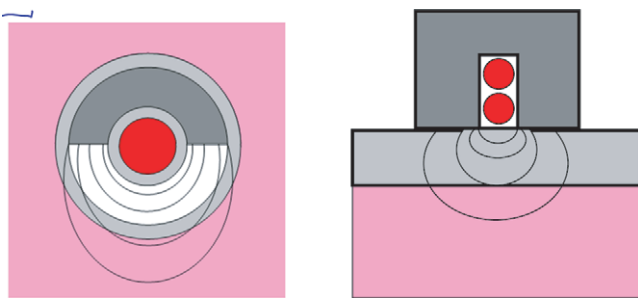


Figure 27. Ineffective FMICP couplers designs.

#### 4.2. FMICPs with an external current channel

In the 1990s, the author used a toroidal-like FMICP with a closed ferromagnetic core to obtain uniform plasma in the chamber. The concept of this FMICP source is shown in figure 28. Two U-shaped quartz tubes were mounted on the top flange of the cylindrical chamber as shown in figure 29. The tube diameter was 5 cm, the chamber diameter was 20 cm and its height 10 cm. Each tube was surrounded by two toroidal ferrite cores (not shown in these figures) with  $\mu = 2000$ , the outer diameter 8.8 cm, inner diameter 5.5 cm and height 1.27 cm. The tubes can also be made of metal, as shown in figure 30, provided that they are electrically insulated from the metal top flange, in order to prevent shortening the discharge current inside the tubes.

The primary windings on the ferrite toroids were driven with 400 kHz rf power inducing discharge current in the U-shaped tubes that closed within the chamber. This kind of FMICP was operated in argon gas at pressures between 1 and 100 mTorr in the power range 20 and 200 W. The plasma in the chamber was maintained partly by the discharge current flowing within the chamber and mainly by plasma diffusion from the opening at the ends of the tubes.

In spite of excellent power transfer efficiency found in this FMICP, ranging between 86% and 98% (depending on rf power and argon pressure), its overall plasma efficiency

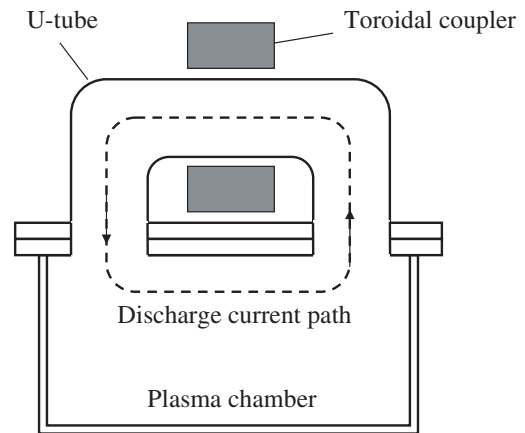


Figure 28. Schematic diagram of FMICP with external current channel.



Figure 29. FM ICP with Quartz tubes.



Figure 30. FMICP with metal tubes.

was disappointingly low. Probe measurement showed that the plasma density in the chamber was an order of magnitude lower than on the tube axis. Moreover, it can be shown that the rf power dissipated in the external current channels localized in the tubes was considerably larger than in the chamber. In other words, the rf power delivered to the toroidal ferrite couplers was mainly spent to maintain plasma in the tubes, which is

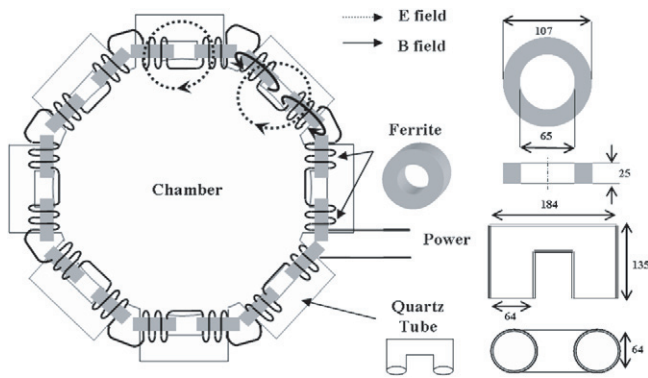


Figure 31. Schematic diagram of the multi-channel FMICP source.



Figure 32. View of the multi-channel FMICP with burning plasma.

converted to radiation and particle loss to the tube wall. Note that the plasma lost in the tube wall is about  $l/r$  times larger than the plasma diffused to the chamber. Here  $l$  is the length of the discharge path in the U-tube which for this kind of FMICP is always significantly larger than the tube radius  $r$ .

A similar topology of external current channels has been utilized for a large processing chamber [56] by setting eight quartz U-tubes (similar to those in figure 29) on the chamber side as shown in figures 31 and 32. This FMICP has operated in argon gas at 400 kHz with the input power between 100 W and 3 kW.

A large power factor close to unity and a low plasma potential close to the floating potential were demonstrated in this FMICP [56]. The power transfer efficiency for various powers and gas pressures is shown in figure 33. The efficiency is over 95%, when the input power exceeds a few hundred watts, which is quite typical for powerful FMICPs with closed magnetic path ferromagnetic couplers.

With 16 plasma injection openings on the chamber circumference, this side-type FMICP has a good plasma density azimuthal symmetry. The plasma density radial distribution measured with a Langmuir probe is shown in figure 34. The shape of the plasma density distribution changes from concave at low rf powers to convex at large rf powers. Control of the radial plasma density distribution for this type of FMICP can be achieved by placing an additional spiral antenna coil (with no ferrite core) driven at 13.56 MHz on the top window [57].

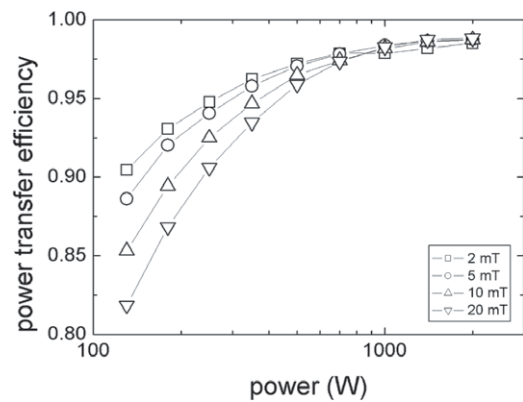


Figure 33. Power transfer efficiency versus power for different argon pressures.

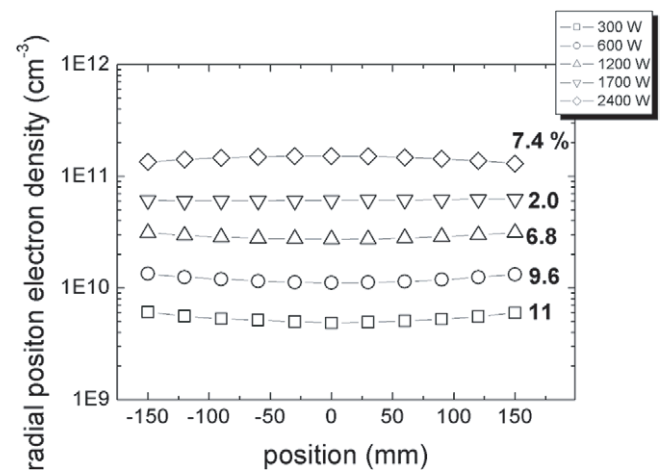


Figure 34. Plasma radial profile. The numbers show plasma non-uniformities.

A plasma reactor in a cylindrical chamber of 90 cm length and 23 cm diameter, with an external channel current maintained in a 4 cm diameter U-shaped tube, has been reported in [58]. This FMICP was intended for treatment of stainless steel and titanium samples. The FMICP operated in nitrogen gas at 0.3 Torr, at 100 kHz with maximal rf power of 5 kW. The plasma density and electron temperature were measured with a double floating probe. However, the maximal electron temperature of 13 eV at 0.3 Torr obtained in [58] makes the result of those probe measurements questionable.

#### 4.3. Distributed FMICPs utilizing closed ferromagnetic cores

Demands for larger processing areas and higher processing uniformity led to proposals (mainly in the patent literature) to distribute several rf couplers over the processing area. In a typical approach, two co-centric antenna coils of different diameters are individually energized to control rf power injection to central and peripheral areas of the plasma. Similarly, distributed power deposition can be achieved with arrays of rf couplers enhanced with ferromagnetic cores.

A distributed FMICP source [14] is shown in figures 35 and 36. Two arrays, consisting of 6 (the inner array) and 12 (the peripheral array) toroidal couplers, are encapsulated

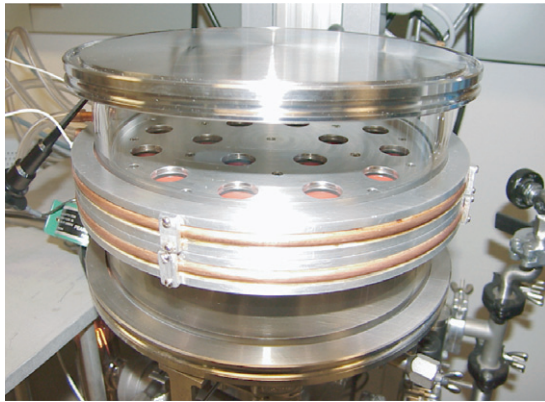


Figure 35. 18 couplers distributed FMICP source.

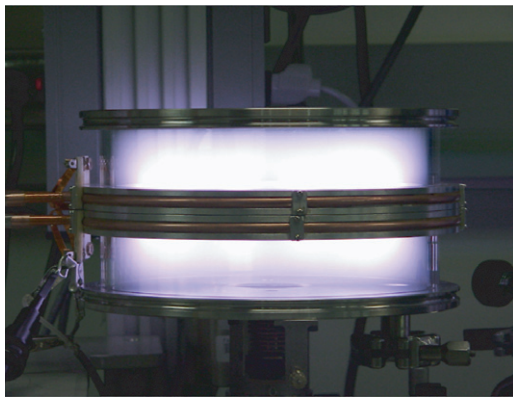


Figure 36. Side view of distributed FMICP source.

in a coupler holder that divides the discharge chamber into two parts. The FMICP is maintained in two half-chambers by discharge current circulating in the opening of neighbouring toroidal couplers. The primary windings of the inductors were connected in series to the rf power sources operated at 400 kHz. The connections of the primary windings were arranged in such a way that the electromotive forces induced in the neighbouring inductors had opposite directions. This enabled closed-path discharge currents to flow through openings in the neighbouring toroidal inductors. The discharge chamber, filled with xenon gas, consisted of two glass tubes (ID = 20 cm) divided by the holder with ferromagnetic inductors and closed at the ends by standard NW-200 stainless steel flanges. The gaps between the holder and flanges were  $h = 4.0$  or  $4.7$  cm. This kind of distributed FMICP operated in the pressure range between 0.3 mTorr to a few Torr. More details on this experiment can be found in [14].

The primary voltage  $V_1$  of 18 couplers connected in series and the apparent power  $P_a = I_1 V_1$  are shown in figure 37 as functions of gas pressure at fixed total power  $P = 400$  W. In the gas pressure range between 1 and 100 mTorr, the voltage (which is proportional to the plasma rf field) changes from about 300 to 100 V, while the primary current changes from 1.33 to 1.0 A. A remarkably large  $\text{Cos}\phi = P/P_a$  ranging between 0.95 and 0.97 reflects an essential resistive input impedance of this FMICP.

Figure 38 shows the power loss in the multiple couplers (which is mainly in the ferrite cores) as a function of the

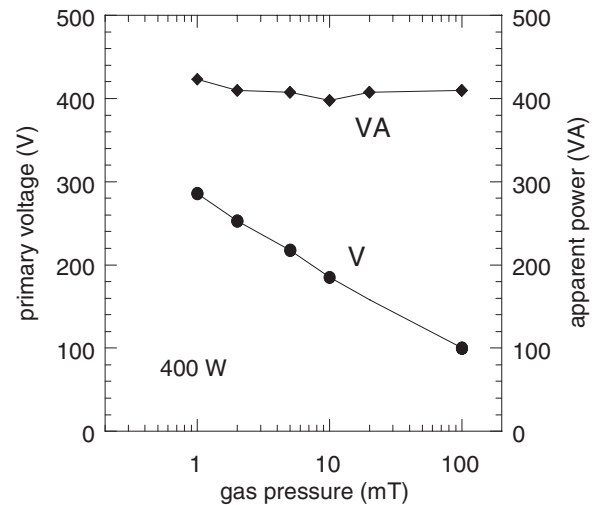


Figure 37. Input voltage and apparent power of distributed FMICP source.

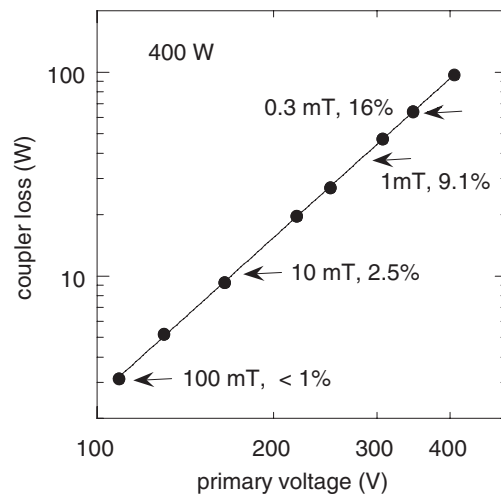
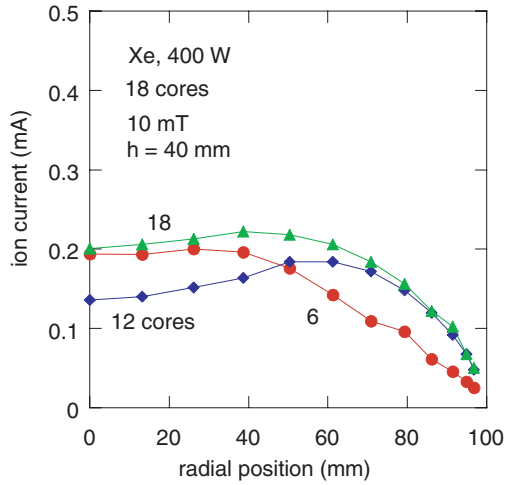


Figure 38. Coupler power loss in distributed FMICP source.

primary voltage. Note the extremely low relative power loss  $\tau$  ranging between 0.75% at 100 mTorr and 16% at 0.3 mTorr of this device. For this particular FMICP, the relative power loss is expected to be somewhat higher in argon gas and significantly higher in the processing molecular gas mixtures due to their high resistivity. However, a high  $\text{Cos}\phi$  and low  $\tau$  can be achieved in a FMICP with processing gases, with a proper FMICP system design provided. Note that the demonstrated values for  $\text{Cos}\phi$  and power transfer efficiency  $\eta = (1 + \tau)^{-1}$  are higher than those in electrical equipment operating at line frequency.

A detailed study of plasma parameters has been performed at 10 mTorr and 400 W. The plasma density measured at the plasma axis in the middle between the holder and the upper flange was  $4.7 \times 10^{11} \text{ cm}^{-3}$  and about half of this value at 2 mm from the top flange, while the EEDF was essentially Maxwellian with the temperature of 2.2 eV. The radial distribution of the ion current to the probe measured near the top flange surface is shown in figure 39 for different combinations of energized coupler arrays. This clearly demonstrates the ability for plasma profile control. Controlling



**Figure 39.** Ion current to probe at the chamber bottom for different numbers of energized couplers.

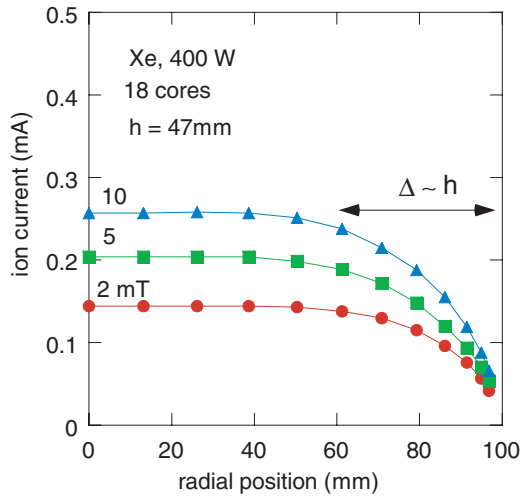


**Figure 40.** The same as in figure 39 for other gap size adjusted to obtain uniform plasma.

the plasma profiles is necessary for uniform plasma processing, rather than achieving plasma uniformity, as we will discuss later. By changing the gap  $h$  between the coupler holder and upper flange, and with series connection of all couplers, one can obtain rather uniform plasma profile as shown in figure 40. The same result (as well as desirable plasma profiles) can be achieved by driving different currents in each array from separate power sources, or from some power distributor.

#### 4.4. Plasma uniformity self-control

Due to strong coupling between the closed-path magnetic core couplers and the associated surrounding plasma, the impedance (that is essentially resistive) of the primary winding of each coupler  $R_k$  is inversely proportional to the local plasma density  $n_k$ , ( $R_k = N^2 R_{pk}$ , and  $R_{pk} \propto n_k^{-1}$ ). By evenly arranging several ferromagnetic inductors with their primary windings connected in series to the rf power source, the rf power deposited to the plasma near each inductor  $P_{dk}$  is inversely proportional to the local plasma density,  $n_k$ :

$P_{dk} = I_1^2 R_k \sim n_k^{-1}$ . This means that a local decrease in plasma density (for whatever reasons: wall proximity and/or a reduction in gas pressure due to gas flow or/and heating) results in a local increase in the rf power deposition. This negative feedback equalizes the plasma density distribution over a processing area. The same mechanism of negative feedback equalizes the plasma density along the positive column of a linear dc discharge.

There are many ways to distribute ferromagnetic inductors over a processing area. Arranging them along a circle provides azimuthally symmetric plasma, while arranging them in a few concentric circles enables a radial control of plasma density. Connecting in series the concentric groups of the couplers provides self-control of the plasma density uniformity in the radial direction. Apparently, more uniform plasma can be achieved with more ferromagnetic inductors distributed over the processing area. The described distributed FMICP source has an internally built-in structure with many openings which could pose some inconvenience, unless the two-wafer processing in this device is considered as a merit.

Owing to the negative static volt–ampere characteristic of the gas discharge plasma ( $dI/dE < 0$ ), individual discharge channels cannot be stable when connected in parallel to a common power source, unless a certain ballasting impedance is included in each channel. In a CCP, the rf sheaths near the electrodes perform the ballasting function locally, thus providing plasma uniformity over the electrode surface. In an ICP, the integral ballasting of the plasma is provided by a leakage inductance of the antenna coil due to its weak coupling with plasma. The utilization of transformer coupling in a multi-inductor DFMICP array with primary windings connected in series allows not only for a stable drive of parallel currents in the plasma, but it also provides self-controlled plasma uniformity.

#### 4.5. What makes efficient ICP source

It is apparent that in order to increase the ICP efficiency and to make it operable at low rf powers and low plasma densities, one has to increase the coupling coefficient. The coupling coefficient is defined not only by the thickness of the window separating the coupler from plasma, but also by the coupler configuration itself. Thus, using a single-turn antenna (to reduce the coupler voltage and undesirable capacitive coupling) results in a significant sacrifice in the coupling and ICP efficiency. This can happen in two ways. First, the rf electric field induced on the surface of the coupler single conductor spatially decays as about  $a/r$ . Since the window thickness  $w$  is usually larger than the conductor radius  $a$ , the power deposition at the skin layer at the plasma boundary is reduced by about  $(w/a)^2$  times, (which is order of 10) compared with the case when an antenna is in contact with the plasma). The second reason is the increase in the power lost in the antenna due to reduction of its  $Q$ -factor  $Q_0 = \omega L/R_w$ . The reduction in the number of turns  $N$  leads to the reduction of  $Q_0$ , since  $L \propto N^2$ , while  $R_w \propto N$ . This holds for not too many turns, when rf current caused by the coil stray capacitance is negligible compared with the coupler current  $I_1$ .

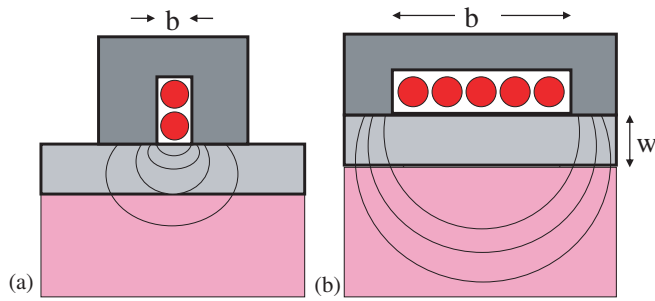


**Figure 41.** Inefficient (a) and efficient (b) ferromagnetic coupler design.

Similar considerations are fully applicable to couplers enhanced with ferromagnetic cores [9, 12, 34, 54, 55] described in section 4.1. The fundamental limitation of these types of FMICP (shown in figure 27) is caused by their structure which consists of a thin antenna conductor partly surrounded by a ferromagnetic shield core. In fact, such structure provides magnetic field augmentation in the small zone between the coupler poles, but most of the rf magnetic flux is closed upon itself within the window and does not reach the plasma.

In order to couple effectively to the plasma, the magnetic flux created by the antenna (coupler) has to embrace the nearby plasma. Figure 41 shows schematically the structure of rf magnetic lines in the FMICP considered in [9, 12, 34, 54, 55], where only a small portion of rf magnetic lines embraces the nearby plasma. To create efficiently an electromotive force which drives the plasma current, the coupler has to produce a magnetic flux that embraces the plasma, rather than just creating a strong rf magnetic field near the coupler itself. This is shown schematically in figure 41(b). In practice, to achieve this important requirement for efficient ICP operations (with and without ferromagnetic core), the coupler (antenna) has to be spread over the window such that the coil width  $b$  be larger, and preferably much larger than the window thickness  $w$ , i.e.  $b \gg w$ .

### 5. Distributed FMICP with flat windows and open ferrite couplers

As stated before, a thin window ( $w \ll b$ ) is one of the key factors for achieving a high efficiency distributed FMICP, which has been designed and reported in [59]. With the thickness of the dielectric window an order of magnitude smaller than the conventional ICP reactors, the coupling of the antenna coil to the plasma is considerably enhanced for this FMICP. Figure 42 (figure 1 in [59]) shows the design idea of the antenna block, which is the top part of the ICP chamber. figure 43(a) (figure 2(a) in [59]) shows a photo of the assembled antenna block, looking from the plasma side. Figure 43(b) (figure 2(b) in [59]) is a photo of the antenna block without the support flange, support ring and the windows. More detailed description on the design consideration of such an antenna block, the movable in the axial direction disc pedestal and the associated Langmuir probes can be found in [59].

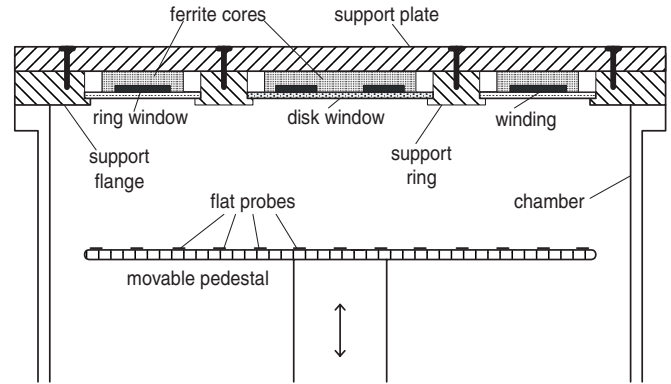


**Figure 42.** Schematic diagram of distributed FMICP chamber with the antenna block and the pedestal. From [59].

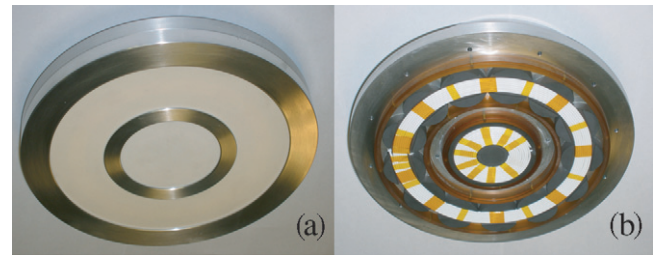


**Figure 43.** Bottom view of the assembled antenna block (a), and that without windows (b). From [59].

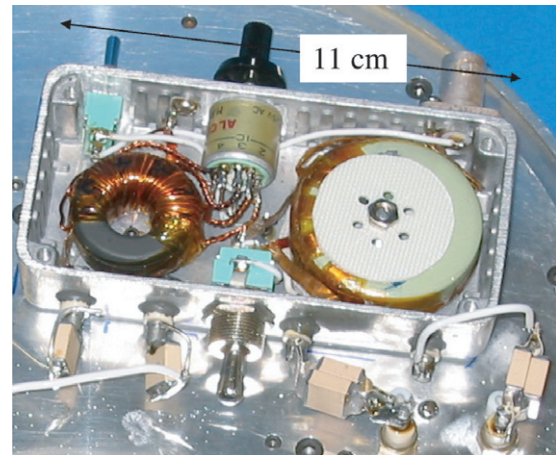


**Figure 44.** Dual matching network.

The experiments were performed with argon gas in this FMICP with a single outer symmetrically driven coil at the fixed frequency of 2 MHz using a dual symmetrical matching network shown in figures 44 and 45 (for more details see [59]). A compact and highly efficient (about 99%, due to the use of a transmission line transformer) matching network provides a true symmetric drive with a weak detuning effect caused by the differences in the plasma load. This occurs due to a relatively small  $Q$ -factor of the coupler loaded with plasma.

Due to utilization of low driving frequency, the symmetrical coupler drive and the window with a high dielectric constant ( $\epsilon_r = 10$ ), that behaves at rf almost as a metal, thus acquires a virtual ground potential, the rf plasma potential was found always to be much lower than the electron temperature measured in this experiment. The low plasma

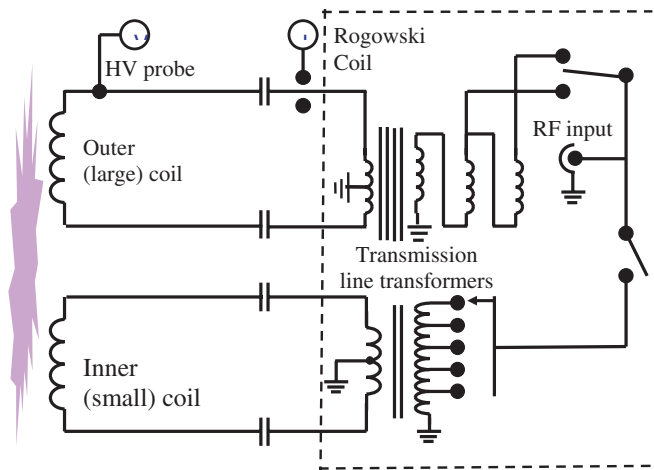


Figure 45. Circuit diagram of the dual matching network.

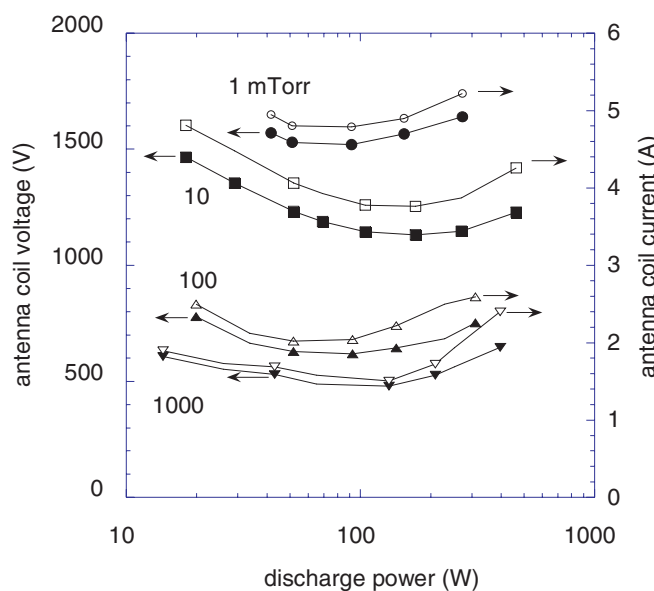


Figure 46. Coupler voltage and current versus discharge power. From [59].

rf potential ensures that the dc voltage in the sheath between the chamber and the plasma, and the dc voltage between the unbiased pedestal and the plasma are minimal and equal to the floating potential.

Figure 46 (figure 5 in [59]) shows the dependence of both coupler voltage and current on the discharge power at different gas pressures (1, 10, 100 and 1000 mTorr). The falling dependence of the coil voltage and the coil current with respect to the discharge power looks strange and suggests decreasing discharge power for increasing coil voltage and current. Such a counterintuitive behaviour of ICP electrical characteristics is due to the strong antenna coupling to plasma and a negative  $V-A$  characteristic of the non-equilibrium gas discharge plasma. At relatively high discharge power (100 W and higher), both the antenna voltage and the current are growing with discharge power. Such behaviour, common for ICP sources, is due to final antenna leakage inductance.

The measured power transfer efficiency  $\eta$  for this FMICP (that also includes the losses in the matching network) is

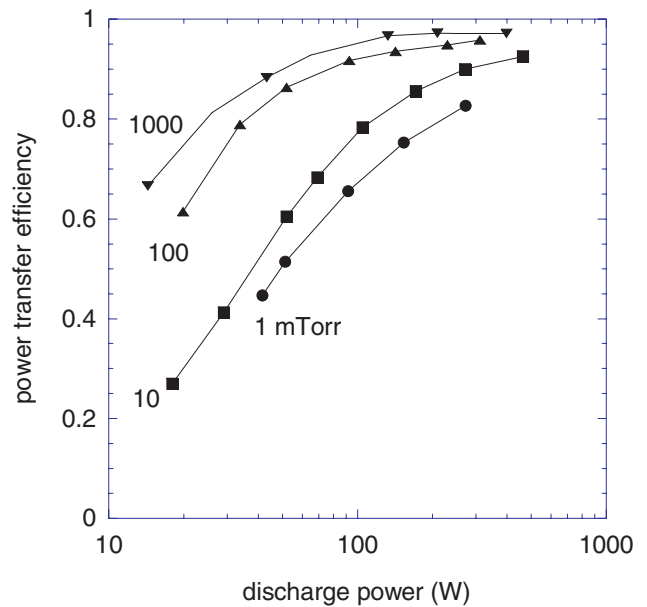
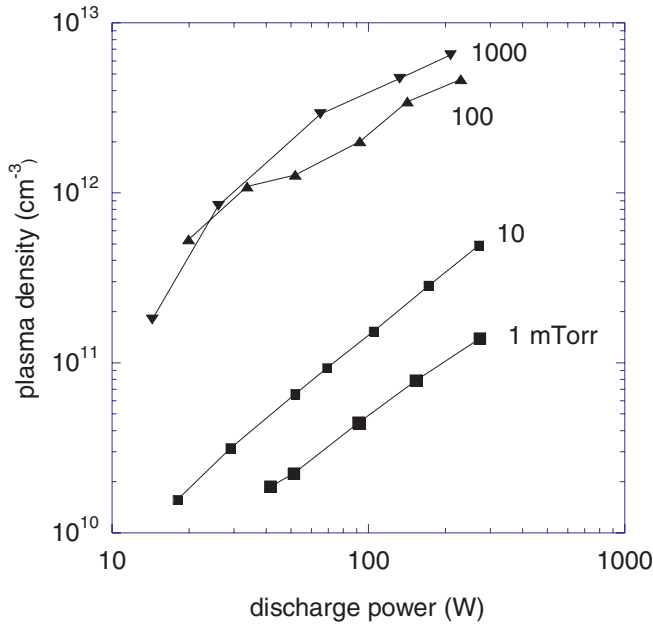


Figure 47. Power transfer efficiency. From [59].

shown in figure 47. The values of  $\eta$  grow monotonically with power (plasma density) and gas pressure, and are considerably larger than in conventional ICP with pancake coil in the same chamber and the plasma parameters. In fact, at discharge power 200 W, the argon pressure between 1 and 1000 mTorr, and the driving frequencies 3.39, 6.78 and 13.56 MHz, the power transfer efficiency was found to be between 0.6 and 0.8, which corresponds to 40% and 20% power loss in the antenna coil. The power transfer efficiency measured in this FMICP at 2 MHz, at the same power and gas pressure demonstrated in figure 47, shows the corresponding numbers between 0.79 and 0.97 which correspond to 21% and 3% power loss in the antenna together with the matching transformer. This considerable difference in the coupler power loss, which is even larger for higher discharge powers, is due to the improved antenna coupling by using the thin window and the application of a ferromagnetic core. More details on comparing efficiencies of FMICP and ICP with identical plasmas can be found in [59]. Significantly lower power dissipated in the coupler is totally due to the enhanced coupling between the coupler and the plasma, with the thin window and the utilization of a suitable ferromagnetic core.

The basic plasma parameters, the electron temperature and the plasma density is found as appropriate integral of the measured EEDFs using a VGPS<sup>®</sup> probe station [61]. Figure 48 shows the plasma density measured over a wide range of argon pressures and discharge powers at the centre of the discharge gap. Here one can observe a wide range of plasma density values covering almost three orders of magnitude including a relatively low plasma density at the lowest discharge power of 15–20 W. In this experiment, the maximal values of the plasma density are limited by the available rf power source. The ability to maintain the plasma at low rf powers (low plasma density) is due to the strong coupling between the antenna and the plasma, and a relatively low power loss in the rf coupler itself.

A stable discharge in this FMICP can be maintained (except at very low gas pressures) over various gap distances,



**Figure 48.** Plasma density versus discharge power for different argon pressure. From [59].

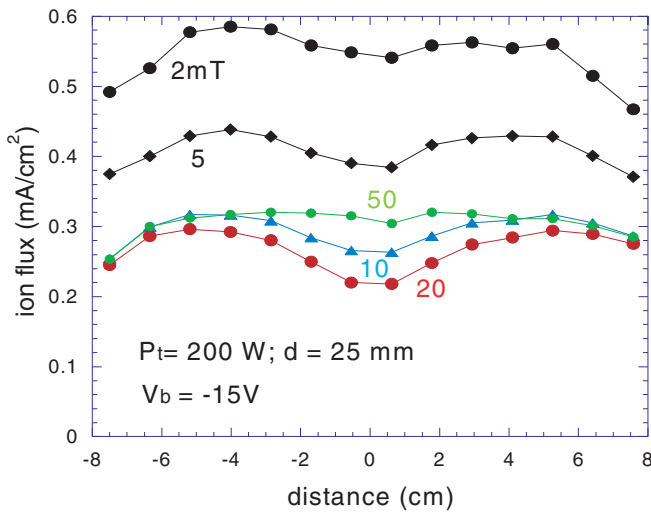


**Figure 49.** Ion current distribution at different argon pressure.

ranging from 1.5 to 8 cm. The discharge gap  $d$  significantly affects the plasma distribution in the radial direction. When  $d$  is large, the plasma has a diffusion-like distribution with a central maximum. When  $d$  is small, the plasma has a bimodal distribution with a central minimum. Figure 49 shows an example of such plasma density distributions [59]. With argon pressures between 2 and 50 mTorr,  $d = 2.5$  cm and  $P_{\text{tr}} = 200$  W, the plasma density distributions have two local maxima in the radial direction. Their locations are shifted to the centre from the radius of the coupler coil (7.5 cm). This non-uniformity can be readily mended by activating a second coupler near the plasma axis, as shown in figure 43(b).

The ability to control the plasma radial distribution with activation of the central coupler is demonstrated in figure 50. In this experiment, the antenna block and the pedestal with the flat probes were installed on the chamber of a larger diameter

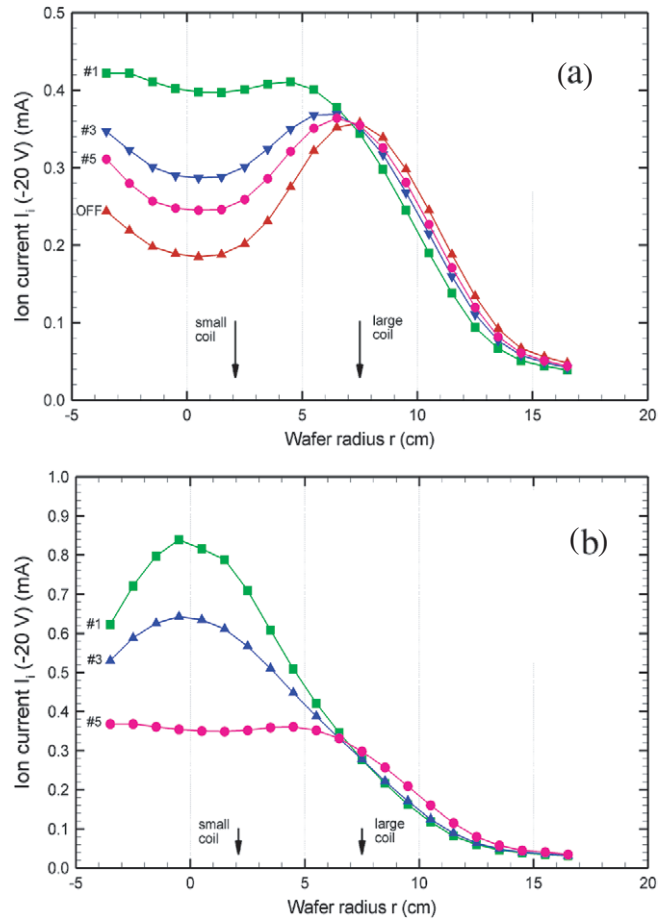


**Figure 50.** Ion current distribution at different power ratio delivered to the couplers.

(40 cm). At a fixed total rf power of 300 W delivered to both couplers, the portion of the power fed to the central coupler is controlled by the switching of the number of turns of the primary winding of the balanced transformer shown in figure 45. A considerable variation in the radial distribution of the ion flux to the pedestal, from concave to convex distribution, is seen in figure 50.

An experiment to control the plasma profile, in a commercial ICP etcher with a peripheral antenna operating at 13.56 MHz, by adding a central antenna with ferromagnetic core driven at 2 MHz has been reported in [62]. Figures 51(a) and 51(b) show, correspondingly, the antenna block with two couplers, and the ion flux profile measured at the wafer at different rf powers (0, 250 and 400 W) fed to the central coupler with ferromagnetic core. The etch rate non-uniformity (ERNU) was also measured in this experiment, and the corresponding numbers are shown in figure 51(b).

The most uniform ion flux over the 300 mm wafer area seen in figure 51(b) is obtained without activation of the central coupler. However, in this case, the etch rate non-uniformity (16%) is much larger than that with energized central coupler, when the ion flux distribution is essentially non-uniform. The best in figure 51(b) ERNU is 2.2% that corresponds to a non-uniform ion flux distribution. The result of this experiment clearly shows that for the uniform etching of large substrates

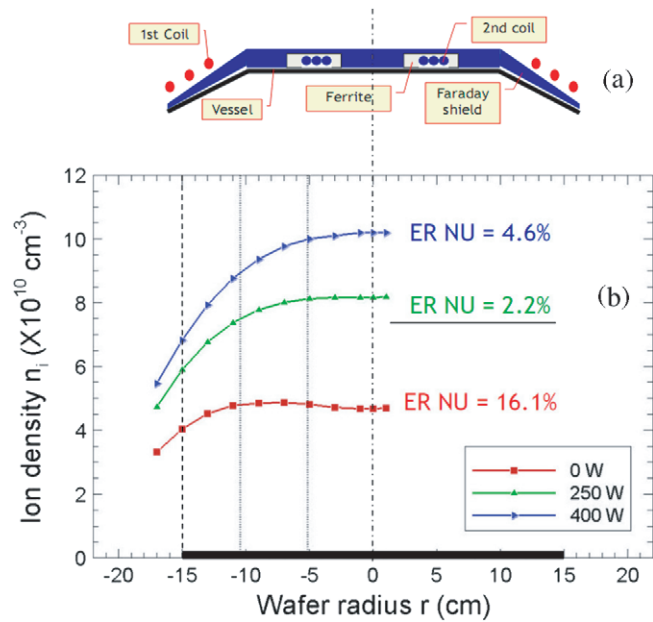


**Figure 51.** Dual couple antenna block (a), and ion current distribution and etch rate non-uniformity at different power delivered to the central coupler (b).



**Figure 52.** Immersed FMICP coupler.

a uniform plasma density distribution is not required, but a controllable plasma density distribution.

The combination of a narrow window and a coupler enhanced by a ferromagnetic core has improved not only the antenna coupling to the plasma, but also the electrical characteristic of the FMICP itself. As a result, the coupler current was decreased, while the power transfer efficiency and the power factor  $\text{Cos}\phi$  were essentially increased, compared with a traditional ‘pancake’ configuration ICP. The lowering of the operation frequency to 2 MHz and using a true balanced drive for the coupler coil resulted in practical elimination of capacitive coupling, and thus removed all negative effects associated with it.

In contrast to the widespread opinion that an ICP cannot work at low plasma densities and with a small gap, these experiments demonstrate the ability of the FMICP to operate over a wide range of gas pressures and plasma densities, including plasma densities considerably lower than  $10^{11} \text{ cm}^{-3}$ , and at small gaps as narrow as 1.5 cm.

The reduction in the window thickness and concentrating of rf magnetic field with ferromagnetic core also results in more local plasma electron heating, thus considerably improving spatial selectivity of the plasma generation and the ability to control the plasma density distribution in a multi-coupler FMICP.

## 6. FMICPs with immersed couplers

A compact plasma (ion) source based on FMICP with an immersed ferromagnetic coupler has been developed and studied in detail by the author and will be published elsewhere. Here, we present some characteristics of this plasma source to demonstrate a missing opportunity that proved to be successful in application for lighting technology considered in section 2.

The concept of this kind of FMICP is similar to that of Bethenod lamp [25] that has been successfully realized in a variety of commercial rf fluorescent lamps. A coupler with a tubular ferrite core having an inner copper thermo-conductor connected to a heat sink is cooled by a fan as shown in figure 52. The coupler is covered with a Pyrex re-entrant cavity which is sealed into a flange connecting the coupler to a cylindrical chamber with diameter of 10 cm and length of 12 cm. The coupler is driven at 2.5 MHz with a simplest matching-tuning network consisting of only a single capacitor tuning the coupler to driving frequency. The FMICP operates in the power range 25–600 W in the range of argon gas pressure between 1 mTorr and 1 Torr.

In this pressure range and the input power of 200 W, the input resistance of the coupler loaded with plasma changed between 20 and 60  $\Omega$ , being equal to 50  $\Omega$  at 10 mTorr, thus ensuring the exact matching to the power source. The electrical and plasma characteristics measured in this FMICP at a total power 200 W, as a function of argon pressure are shown in figures 53–55.

A high power factor (around 0.4) and a very small relative power loss (less than 2%), at argon pressure 15 mTorr and higher, is seen in figure 54. These numbers are close to corresponding numbers found in the FMICP with closed magnetic path. In general, the effective permeability  $\mu_{\text{eff}}$  of the rod (or tubular) couplers (depending on the core length) is around 10, being somewhere between  $\mu_{\text{eff}}$  of opened cores ( $\mu_{\text{eff}} = 1.5\text{--}2$ ) and those of closed cores ( $\mu_{\text{eff}} = 50\text{--}2000$ ). Correspondingly, the coupling, power factor and relative coupler loss in the immersed core FMICPs has some intermediate, but closer to the values of FMICPs with closed couplers. More details on this kind of FMICP will be published elsewhere.

An operation of this FMICP in the pulse mode is reported in [63]. The pulse mode allows for considerable reduction in

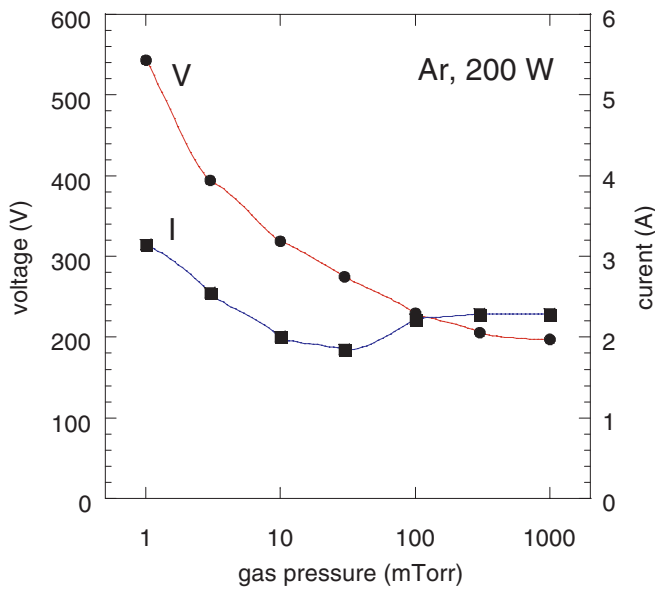


Figure 53. Coupler voltage and current of the immersed FMICP.

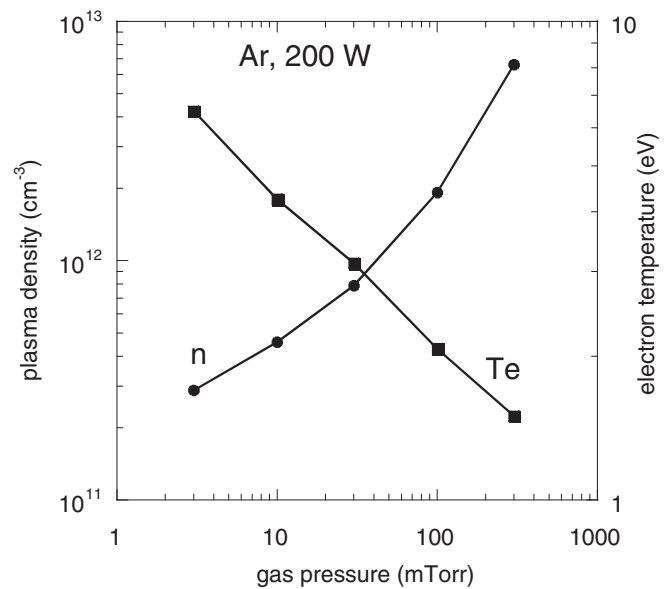


Figure 55. Plasma density and electron temperature.

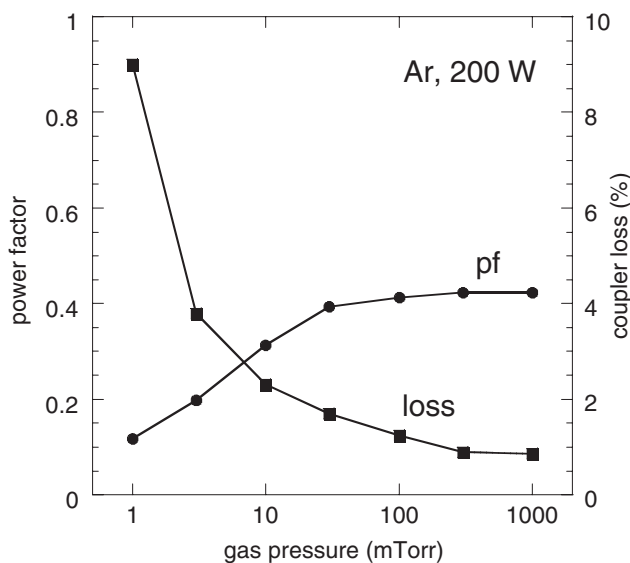


Figure 54. Power factor and coupler power loss versus argon pressure.

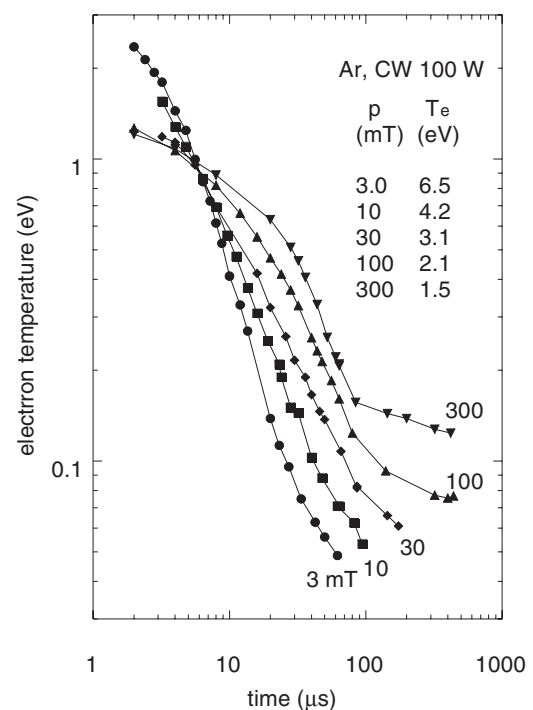


Figure 56. Electron temperature evolution in afterglow stage in immersed FMICP.

the electron temperature in the afterglow stage between the pulses. The electron temperature is found in this experiment by integration of the time-resolved measurement of the EEDF. Evolution of the electron temperature in the afterglow stage is shown in figure 56, demonstrating up to two orders of magnitude drop in the electron temperature.

The operation of this FMICP in the pulse repetitive mode ( $2\ \mu\text{s}$  on and  $20\ \mu\text{s}$  off) showed that, at the same average rf power, the periodically pulsed FMICP has a significantly larger plasma density and lower electron temperature than in a CW mode. To achieve an increase in the averaged plasma density and the electron cooling, a significant (about an order of magnitude) plasma over-powering is required during the pulse. In this respect, FMICPs with their strong coupling to plasma have a serious advantage compared with conventional ICP and CCP sources operating in pulse mode.

Operating closely to a conventional transformer, the FMICPs require the pulse voltage on its couplers nearly proportional to the plasma pulse rf electric field needed for intense ionization during the pulse. Both conventional ICP and CCP are internally ballasted; the first with a considerable leakage inductance of the antenna coil, the second, with electrode rf sheaths. The impedance of the leakage inductance and the impedance of the electrode rf sheaths are nearly independent of discharge power, while the plasma impedance is falling with discharge power. Therefore, to achieve the same increase in the plasma electric field, the ICP and CCP

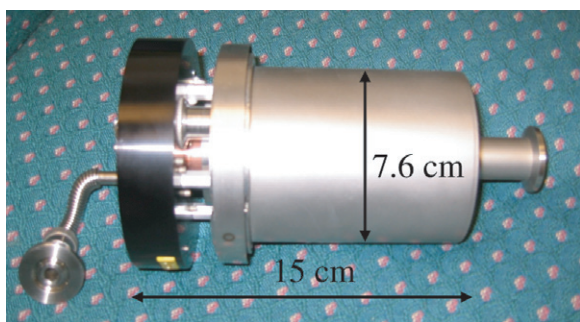


Figure 57. Compact rf cathode.

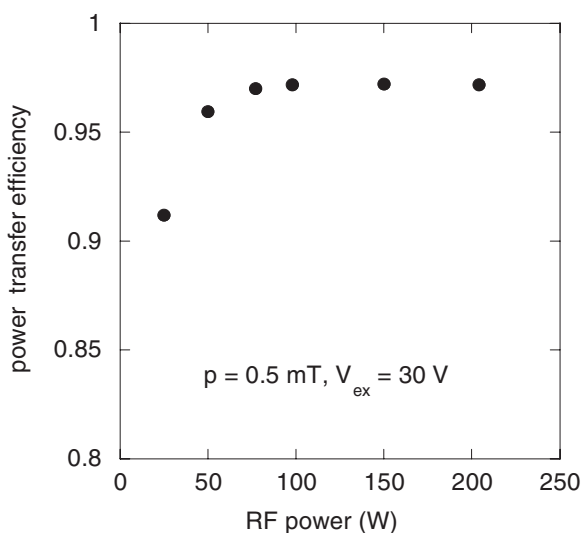


Figure 58. Power transfer efficiency of the rf cathode.

require significantly larger overvoltage than FMICP. Having rather high rf voltages even in the CW mode, the operating of these discharges in the pulse mode would require excessively high rf voltages that may cause significant problems.

Another advantage of using of FMICPs in the pulse mode is a relatively low  $Q$ -factor of their coupler-matching networks,  $Q = (\text{Cos}\phi^{-2} - 1)^{1/2}$ . Considerably larger  $Q$ -factors of conventional ICP and especially that of CCP is the reason for their inability of fast interrupting the discharges due to the ringing of their coupler-matching networks having large  $Q$ -factors. The ringing time of a few microseconds in a pulse-driven CCP at 13.56 MHz has been reported in [64].

A compact plasma cathode for a thruster ion beam neutralization built as an FMICP with immersed coupler is reported in [65]. The plasma cathode consisting of discharge chamber with 7.6 cm OD and 11.5 cm length has an immersed rf ferrite coupler cooled with a cape sink that houses a matching-tuning network and a variety of ports for starting and diagnostics means, is shown in figure 57. The cathode is operated at 2.0 MHz with xenon gases in the power range between 20 and 200 W. The electron beam is extracted from the NW16 pumping port (on the right-hand side in figure 57) to 30 V biased collector.

The power transfer efficiency of this plasma cathode versus the total power delivered to the matching network is shown in figure 58. The efficiency is 97% at 0.5 mTorr xenon

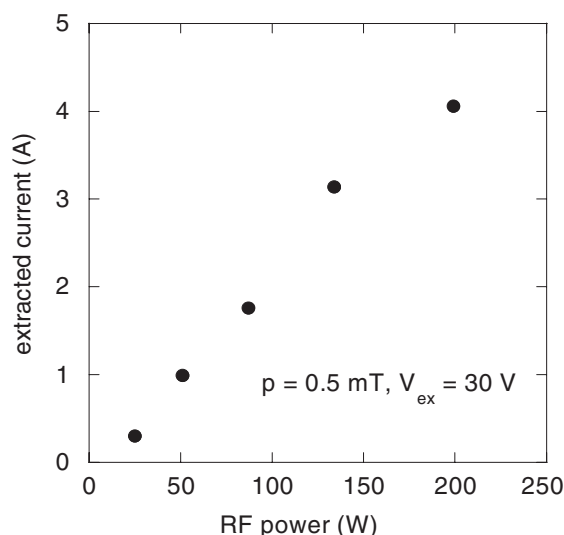


Figure 59. Extracted electron current versus total rf power.

gas downstream pressure, when the power exceeds 70 W. The extracted electron current as a function of the total power is shown in figure 59. The extracted current is nearly proportional to the rf power with the emission efficiency of  $20 \text{ mA W}^{-1}$ , corresponding to the electron production cost of 50 eV. The electron emission efficiency of  $25 \text{ mA W}^{-1}$  was maximal at 2 mTorr of downstream pressure, that considerably exceeds the emission efficiency of  $14 \text{ mA W}^{-1}$  at 60 V extraction voltage obtained in a microwave plasma cathode [66, 67] and of  $12.5 \text{ mA W}^{-1}$  at 80 V extraction voltage obtained in a helicon plasma cathode operating at 13.65 MHz [68, 69]. Apart from higher efficiency the described immersed FMICP is considerably simpler and cheaper than microwave and helicon plasma cathodes. It is apparent that with an appropriate extraction-accelerating system this kind of FMICP can operate as a highly efficient ion source.

## 7. Concluding remarks

In this review, we have considered a variety of FMICP applications and presented a detailed comparative study of their electrical and plasma parameters. We have demonstrated many advantages of these plasma sources compared with conventional ICPs. The introduction of a ferromagnetic core to a magnetic rf circuit of an ICP enhances the coupling and causes the FMICP to operate close to an ideal transformer, thus increasing its efficiency and power factor. This simplifies considerably the FMICP matching to an rf source. Applying a ferromagnetic core also allows for a considerable reduction in the FMICP driving frequency (up to 2–3 orders of magnitude) compared with the standard of 13.56 MHz in the industry. By reducing the operation frequency and using the push-pull drive, one eliminates the capacitive coupling and transmission line effects, inherent to ICP operating at 13.56 MHz. Utilization of lower frequencies also results in more efficient and less expensive rf power sources. Due to strong coupling, the application of FMICP operating in the pulse mode is easier and more reliable than the application of conventional ICP

and CCP sources. One of the features of FMICP, valuable for plasma processing, is its ability to focus rf power injection, which allows for effective control of plasma profiles, which is necessary for uniform plasma processing over large substrate areas.

The experiments presented in this review show that a properly designed FMICP can operate over a wide range of rf power and gas pressure, and it can do everything that other rf and microwave plasma sources can do, but more efficiently and more cost effectively.

## Acknowledgment

This work was partly supported by the DOE OFEC (Contract # DE-SC00019390).

## References

- [1] Hershkowitz N, Ding J, Breun R A, Chen R T S, Mayer J and Quick A K 1996 *Phys. Plasmas* **3** 2197
- [2] Godyak V A 2006 *IEEE Trans. Plasma Sci.* **34** 755
- [3] Lieberman M A and Lichtenberg A J 2005 *Principles of Plasma Discharges and Material Processing* (New York: Wiley)
- [4] Chen F F and Chang J P 2002 *Lecture Notes on Principles of Plasma Processing* (Dordrecht/New York: Kluwer/Plenum)
- [5] Lieberman M A, Booth J P, Chabert P, Rax J M and Turner M M 2002 *Plasma Sources Sci. Technol.* **11** 283
- [6] Chabert P 2007 *J. Phys. D: Appl. Phys.* **40** R63
- [7] Chabert P, Raimbault J L, Levif P, Rax J M and Lieberman M A 2005 *Phys. Rev. Lett.* **95** 205001
- [8] Volynets V, Ushakov A, Lim G, Lim Y, Shin H, Woo J, Kim K and Sung D 2008 *J. Vac. Sci. Technol. A* **26** 406
- [9] Meziani T, Colpo P and Rossi F 2001 *Plasma Sources Sci. Technol.* **10** 276
- [10] Godyak V A 2003 *Presentation at PEUG (Santa Clara, CA, September 2003)*
- [11] Godyak V A 2004 *Proc. 15th Int. Conf. on Gas Discharges and their Applications (Toulouse, France)* vol 2 p 621
- [12] Colpo P, Meziani T and Rossi F 2005 *J. Vac. Sci. Technol. A* **23** 270
- [13] Chen F F, Evans J D and Tynan G R 2001 *Plasma Sources Sci. Technol.* **10** 236
- [14] Godyak V A and Chung C-W 2006 *Japan J. Appl. Phys.* **45** 8035
- [15] Lim J H, Kim K N, Park J K and Yeom G Y 2008 *J. Korean Phys. Soc.* **52** 313
- [16] Godyak V A 2002 *IEEE Industry Appl. Mag.* **42**
- [17] Boulos M I 1985 *Pure Appl. Chem.* **57** 1321
- [18] Eckert H U 1984 *2nd Annual Int. Conf. on Plasma Chemistry Technology (San Diego, CA)* p 171
- [19] Hopwood J 1992 *Plasma Source Sci. Technol.* **1** 109
- [20] Keller J H 1997 *Plasma Phys. Control. Fusion* **39** A437
- [21] Godyak V A 2003 *Plasma Phys. Control. Fusion* **45** A399
- [22] Godyak V A 2005 *Phys. Plasmas* **12** 3553
- [23] Kral'kina E A 2008 *Usp. Fiz. Nauk* **178** 519
- [24] Chabert P and Braithwaite N 2011 *Physics of Radio-Frequency Plasmas* (Cambridge: Cambridge University Press)
- [25] Bethenod J and Claude A 1936 *US Patent* 2,030,957
- [26] Netten A and Verheij C M 1991 *Operating Principles of the Philips QL Lamp System* (Eindhoven: Philips Lighting V. G.)
- [27] Green B J 2003 *Plasma Phys. Control. Fusion* **45** 687
- [28] Bell W E 1965 *Appl. Phys. Lett.* **7** 190
- [29] Anderson J M 1969 *Trans. (April) IES* 236
- [30] Godyak V A and Schaffer J 1998 *Proc. 8th Int. Symp. on Sci. and Technol. of Light Sources (Greifswald, Germany)* p 14
- [31] Statnic E 2004 *Proc. 10th Int. Symp. on Sci. and Technol. of Light Sources (Toulouse, France)* p 287
- [32] Kogan V A and Ulanov I M 1993 *High Temp.* **31** 129
- [33] Smith D K, Chen X, Holber W M and Georgelis E 1998 *US Patent* 6,150,628
- [34] Lloyd S, Shaw D M, Watanabe M and Collins G J 1999 *Japan. J. Appl. Phys.* **38** 4275
- [35] Shaffer J and Godyak V A 1999 *J. Illum. Eng. Soc.* **28** 142
- [36] Godyak V A, Piejak R B and Alexandrovich B M 1999 *Proc. 9th Int. Symp. on the Science and Technology of Light Sources (Cornell University, Ithaca, NY)* p 157
- [37] Alexandrovich B M, Godyak V A and Lister G G 2004 *Proc. 10th Int. Symp. on the Science and Technology of Light Sources (Toulouse, France)* p 283
- [38] Lister G G, Lawler J E, Lapatovich W P and Godyak V A 2004 *Rev. Mod. Phys.* **76** 541
- [39] Wharmby D O 1997 *Lamp and Lighting* (New York: Wiley) p 216
- [40] Godyak V A, Alexandrovich B M, Sapozhnikov A A and Speer R 2007 *Proc. 11th Int. Symp. on the Science and Technology of Light Sources (Shanghai, China)* p 377
- [41] Reinbeg A R, Steinberg G N and Zarowin C B 1984 *US Patent* 4,431,898
- [42] Hiramatsu K and Takamura S 1992 *Japan. J. Appl. Phys.* **31** 2243
- [43] Watanabe Y and Ohta K 2002 *Proc. ESCAMPIG16 (Grenoble)* p 245
- [44] Zhang B C and Cross R C 1998 *Rev. Sci. Instrum.* **69** 101
- [45] Zhang B C and Cross R C 1998 *J. Vac. Sci. Technol. A* **16** 2016
- [46] Ulanov I M and Isupov M V 2010 *Applied Physics in the 21st Century* (New York: Nova Science Publishers) p 113 chapter 3
- [47] Bliokh Yu P, Feisteiner J, Slutsker Ya Z and Vaisberg P M 2004 *Appl. Phys. Lett.* **85** 1484
- [48] Eckert H U 1974 *IEEE Trans. Plasma Sci.* **2** 308
- [49] Piejak R B, Godyak V A and Alexandrovich B M 1992 *Plasma Sources Sci. Technol.* **1** 179
- [50] Godyak V A, Piejak R B, Alexandrovich B M and Kolobov V I 1998 *Phys. Rev. Lett.* **80** 3264
- [51] Lieberman M A and Godyak V 1998 *IEEE Trans. Plasma Sci.* **26** 955
- [52] Godyak V A 1998 *Electron Kinetics and Application of Glow Discharges* (New York: Plenum Press) p 241
- [53] Shinohara S, Miyauchi Y and Kawai Y 1995 *Plasma Phys. Control. Fusion* **37** 1015
- [54] Lim J H, Kim K N, Gweon G H and Yeom G Y 2009 *J. Phys. D: Appl. Phys.* **42** 015204
- [55] Lim J H, Kim K N, Gweon G H, Hong S P, Kim S H and Yeom G Y 2010 *J. Phys. D: Appl. Phys.* **43** 095202
- [56] Lee K, Lee Y, Jo S, Chung C-W and Godyak V A 2008 *Plasma Sources Sci. Technol.* **17** 015014
- [57] Bang J-Y, Kim J-Y and Chung C-W 2011 *Phys. Plasma* **18** 073507
- [58] Ulanov I M, Isupov M V, Aleshina L A, Glazkova S V and Loginov D V 2012 *7th Int. Conf. on Plasma Technology (Minsk, Belarus)* vol 1 p 208
- [59] Godyak V A 2011 *Plasma Sources Sci. Technol.* **20** 025004
- [60] Godyak V A, Piejak R B and Alexandrovich B M 1999 *J. Appl. Phys.* **85** 703
- [61] [www.plasmasensors.com](http://www.plasmasensors.com)
- [62] Nagorny V P and Lee D 2011 *ISPC 20 (Philadelphia, PA)*
- [63] Godyak V A and Alexandrovich B M 2005 *27th ICPIG (Eindhoven, The Netherlands)* vol 1 p 221

- [64] Pu Y-K 2012 private communication
- [65] Godyak V A, Raitses Y and Fisch N J 2007 *Proc. 30th Int. Electric Propulsion Conf. (Florence, Italy)* p 266
- [66] Diamant K K 2005 *41st Joint Propulsion Conf. and Exhibit (Tucson, AZ)* AIAA 3662
- [67] Diamant K K 2005 *29th Int. Electric Propulsion Conf. (Princeton, NJ)* IEPC 007
- [68] Longmier B and Hershkowitz N 2005 *41st Joint Propulsion Conf. and Exhibit. (Tucson, AZ)* AIAA 3856
- [69] Longmier B, Baalrud S and Hershkowitz N 2006 *Rev. Sci. Instrum.* **77** 113504